THE UNIVERSITY OF MICHIGAN

COLLEGE OF ENGINEERING

Department of Aerospace Engineering
High Altitude Engineering Laboratory

Scientific Report

ADMITTANCE OF THE INFINITE CYLINDRICAL ANTENNA IN A LOSSY PLASMA, III. THE COMPRESSIBLE, MAGNETOPLASMA

Edmund K. Miller

ORA Project 05627

under contract with:

NATIONAL AERONAUTICS AND SPACE ADMINISTRATION

CONTRACT NO. NASr-54(05)

WASHINGTON, D. C.

administered through:

OFFICE OF RESEARCH ADMINISTRATION ANN ARBOR

October 1967

TABLE OF CONTENTS

List of Figures iv

Abstract v

I. Introduction 1

II. Formulation 3

II. 1. The Vacuum Sheath 5

II. 2. The Sheathless Case 17

II. 3. The Inhomogeneous Sheath 21

III. Numerical Results 26

IV. Comparison with Experimental Results 42

V. Conclusion 45

Appendix A 48

References 53

List of Figures

1. The free-space infinite cylindrical antenna admittance as a function of frequency with the exciting gap thickness, δ, a parameter and a radius, c, of 1 cm. 27

2. The infinite antenna admittance as a function of frequency for the compressible, magnetoplasma and the sheathless case with a radius of 1 cm, an electron plasma frequency of 1.5 MHz and electron cyclotron frequency of 1.0 MHz. 28

3. The infinite antenna admittance as a function of frequency for the compressible, magnetoplasma and the sheathless case with a radius of 1 cm, an electron plasma frequency of 1.0 MHz and electron cyclotron frequency of 1.5 MHz. 30

4. The infinite antenna admittance as a function of frequency for the incompressible magnetoplasma and the sheathless case, with an electron plasma frequency of 1.5 MHz and electron cyclotron frequency of 1.0 MHz. 32

5. The infinite antenna admittance as a function of frequency for the incompressible magnetoplasma and the sheathless case, with an electron plasma frequency of 1.0 MHz and electron cyclotron frequency of 1.5 MHz. 33

6. The infinite antenna admittance as a function of frequency in the incompressible magnetoplasma with a vacuum sheath thickness of 5 D_ℓ, an electron plasma frequency of 1.5 MHz and electron cyclotron frequency of 1.0 MHz. 34

7. The infinite antenna admittance as a function of frequency in the incompressible magnetoplasma with a vacuum sheath thickness of 5 D_ℓ, an electron plasma frequency of 1.0 MHz and electron cyclotron frequency. of 1.5 MHz. 35

8. The infinite antenna admittance as a function of frequency in an isotropic plasma for both the compressible ($T=1,500^{o}K$) and incompressible ($T=0^{o}K$) cases and zero sheath thickness with an electron plasma frequency of 1.5 MHz. 37

9. The infinite antenna admittance as a function of frequency in an isotropic plasma for both the compressible ($T=1,500^{o}K$) and incompressible ($T=0^{o}K$) cases and a vacuum sheath thickness of 5 D_ℓ, with an electron plasma frequency of 1.5 MHz. 38

10. The circumferential current as a function of frequency for the compressible magnetoplasma and the sheathless case with an electron plasma frequency of 1.5 MHz and electron cyclotron frequency of 1.0 MHz. 40

11. The circumferential current as a function of frequency for the compressible magnetoplasma and the sheathless case with an electron plasma frequency of 1.0 MHz and electron cyclotron frequency of 1.5 MHz. 41

Abstract

An analysis of the current on an infinite cylindrical antenna which is excited across a circumferential gap of non-zero thickness and immersed in a lossy, compressible, magnetoplasma with its axis parallel to the static magnetic field, is described. Some numerical results are presented for the antenna admittance for the sheathless case, where the uniform magnetoplasma is in contact with the antenna surface. The admittance values are obtained from a numerical integration of the Fourier integral for the antenna current, and are given for plasma parameter values typical of the E-region of the ionosphere.

The admittance results obtained exhibit a maximum slightly above the electron cyclotron frequency (f_h), and in this regard are similar to those obtained when the magnetoplasma is incompressible but separated from the antenna by a free-space layer (the vacuum sheath). The conductance is found to exceed the susceptance except in the frequency range encompassed by the upper hybrid frequency and f_h, which is also approximately the range of inductive susceptance, the susceptance otherwise being capacitive. The admittance is also found to exhibit a minimum or slight kink at the plasma frequency, a feature also found in the imcompressible magnetoplasma results. It is concluded that of the plasma compressibility, plasma anisotropy and the vacuum sheath, taken separately, the latter two exert the strongest influence on the infinite antenna admittance.

A comparison of the theoretical results with experimental measurements of antenna impedance in the ionosphere shows there to be a qualitative similarity in the admittances. In particular, the experimental admittance is found to have a minimum or kink at the plasma frequency, similar to that observed in the theoretical results while an experimental admittance maximum is found above the cyclotron frequency, indicating the influence of a sheath and/or the plasma compressibility.

I. Introduction

With the opportunities now afforded by rocket and satellite experimentation in the ionosphere, there has developed today a great deal of interest in the behavior of plasma-immersed antennas. This is in part due to the necessity for predicting the influence of the ionospheric plasma on telemetry antennas utilized in the rocket or satellite payload. Of as least equal importance however, is the desire to use if possible, an antenna as a diagnostic probe for determining some of the properties of the ambient ionosphere in which it is immersed. The present study has been undertaken with the latter goal in mind in an attempt to gain a better understanding of the relative importance of the various factors which may influence the admittance of an antenna in the ionosphere. Among these factors are acoustical and sheath effects which arise from the non-zero plasma temperature, and the plasma anisotropy resulting from the ionospheric magnetic field.

The antenna geometry chosen for the investigation is that of an infinite, cylindrical dipole driven at a circumferential gap of non-zero thickness, a geometry which allows a rigorous boundary value problem approach to be used. The antenna is oriented with its axis parallel to the static magnetic field in the plasma. The case of the compressible*, isotropic plasma was reported on previously by the author (Miller, 1967a, referred to hereafter as I), and in a subsequent report (Miller, 1967b, referred to hereafter as II) the incompressible, anisotropic plasma was considered. In both I and II the actual sheath which forms about a body at floating potential in a warm plasma was approximated by a concentric, free-space layer between the antenna and the external uniform plasma, a sheath model commonly referred to in the literature as a vacuum sheath.

---

* A "compressible plasma" is used in this report to denote a plasma in which the electron pressure wave, or electrokinetic wave, can propagate.

In the present report, the treatments given in I and II are extended to the more general case of the compressible, anisotropic plasma medium. This means that the antenna can excite three mode types in the plasma, two of which are basically electromagnetic (EM) in nature, and one a basically electron pressure or electrokinetic (EK) wave. Since these waves are coupled as a result of the plasma anisotropy, none of them is purely electromagnetic or electrokinetic. By comparison, two EM modes are encountered in the development of II, while in I there is one EM and the EK mode to be considered. A vacuum sheath model will be considered here in formulating the boundary value problem, but due to the extreme complexity of the numerical calculations, numerical results are given here for the sheathless case only.

A comparison of the admittance results obtained here with those previously given in I and II will be made, in an attempt to demonstrate the relative influence of the various factors considered on the infinite antenna admittance. The relevance of the calculated results to some experimental measurements of antenna impedance in the ionosphere will be discussed. It will be shown that the experimental and theoretical results are in qualitative agreement on some significant features of the admittance variation with excitation frequency. As in I and II, the RMKS system of units will be used unless otherwise specified.

II. Formulation.

The field behavior in the plasma is described by the time-dependent hydrodynamic equations for the electrons (ion motion is neglected) together with Maxwell's equations, as

$$\nabla \times \underline{E}(\underline{r}, t) = -\mu_o \frac{\partial}{\partial t} \underline{H}(\underline{r}, t) \tag{1}$$

$$\nabla \times \underline{H}(\underline{r}, t) = \epsilon_o \frac{\partial}{\partial t} \underline{E}(\underline{r}, t) - q N(\underline{r}, t) \underline{V}(\underline{r}, t) \tag{2}$$

$$\left(\frac{\partial}{\partial t} + \underline{V}(\underline{r}, t) \cdot \nabla\right) \underline{V}(\underline{r}, t) = -\frac{q}{m} \underline{E}(\underline{r}, t) - \nu \underline{V}(\underline{r}, t) - \frac{\nabla P(\underline{r}, t)}{mN(\underline{r}, t)} - \frac{q}{m} \mu_o \underline{V}(\underline{r}, t) \times \underline{H}(\underline{r}, t) \tag{3}$$

$$\left(\frac{\partial}{\partial t} + \underline{V}(\underline{r}, t) \cdot \nabla\right) N(\underline{r}, t) + N(\underline{r}, t) \nabla \cdot \underline{V}(\underline{r}, t) = 0 \tag{4}$$

$$N(\underline{r}, t)\, T(\underline{r}, t)^{-1/(\gamma-1)} = \text{constant} \tag{5}$$

$$P(\underline{r}, t) = k N(\underline{r}, t)\, T(\underline{r}, t) \tag{6}$$

where $\underline{E}$ and $\underline{H}$ are the total electric and magnetic fields, $\underline{V}$, N and P are the macroscopic electron velocity, number density and pressure, -q and m are the electron charge and mass, ν is the electron collision frequency, ϵ_o and μ_o are the permittivity and permeability of free space, and $\underline{r}$ and t are the space and time coordinates. The quantity γ is the ratio of specific heats for the electron gas.

The procedure followed here is the same as that used previously in I and II, in that Eqs. (1) - (6) are linearized by introducing time varying or dynamic perturbation quantities which are small in comparison with the non-time varying or static quantities. Again, since the resulting boundary value problem depends on the sheath model used in the analysis, the vacuum sheath and inhomogeneous sheath models will be treated separately below. The vacuum sheath model is one where the actual sheath is replaced by a free-space layer

which separates the antenna from the external uniform plasma. The inhomogeneous sheath model is one where the actual sheath inhomogeneity is taken into account, and the plasma extends to the cylinder surface. In either case, the sheath is assumed to be of finite thickness and of radius $\rho = s$, forming a concentric layer between the antenna surface of radius $\rho = c$, whose axis is coincident with the z-axis of a cylindrical (ρ, φ, z) coordinate system, and the external uniform plasma. The antenna is assumed to be excited by a circumferential slot of non-zero thickness centered at $z = 0$, across which a voltage $e^{i\omega t}$ which is independent of the azimuthal coordinate φ is applied. Contrary to the isotropic plasma case investigated in I, an azimuthal, as well as an axial antenna current are excited, as a result of the static, axially-directed magnetic field. While the problem is here formulated for the sheathed antenna for the sake of generality, because of the extreme complexity of the numerical calculations, admittance results will be presented for the sheathless case only.

II. 1. The Vacuum Sheath.

In analyzing the vacuum sheath model, Eqs. (1) - (6) are required to describe the fields in the uniform magnetoplasma region external to the sheath, while only (5) and (6) are required for the sheath region itself with $N(\underline{r}, t) = 0$ there. We consider first of all the plasma fields, and linearize (1) - (6) by introducing

$$\underline{E}(\underline{r}, t) = \underline{e}(\underline{r}, t) \tag{7a}$$

$$\underline{H}(\underline{r}, t) = H\hat{z} + \underline{h}(\underline{r}, t) \tag{7b}$$

$$\underline{V}(\underline{r}, t) = \underline{v}(\underline{r}, t) \tag{7c}$$

$$N(\underline{r}, t) = N + n(\underline{r}, t) \; ; \; |n| << |N| \tag{7d}$$

$$P(\underline{r}, t) = P + p(\underline{r}, t) \; ; \; |p| << |P| \tag{7e}$$

$$T(\underline{r}, t) = T + \tau(\underline{r}, t) \; ; \; |\tau| << |T| \tag{7f}$$

so that (1) - (6) become

$$\nabla \times \underline{e}(\underline{r}, t) = -\mu_o \frac{\partial}{\partial t} \underline{h}(\underline{r}, t) \tag{8}$$

$$\nabla \times \underline{h}(\underline{r}, t) = \epsilon_o \frac{\partial}{\partial t} \underline{e}(\underline{r}, t) - q N \underline{v}(\underline{r}, t) \tag{9}$$

$$\frac{\partial}{\partial t} \underline{v}(\underline{r}, t) = -\frac{q}{m} \underline{e}(\underline{r}, t) - \nu \underline{v}(\underline{r}, t) - \frac{\gamma kT}{mN} \nabla n(\underline{r}, t) - \frac{q}{m} \underline{v}(\underline{r}, t) \times (\mu_o H\hat{z}) \tag{10}$$

$$\frac{\partial}{\partial t} n(\underline{r}, t) + N \nabla \cdot v(\underline{r}, t) = 0 \tag{11}$$

Note that the static and dynamic pressures are given by

$$P = kTN$$

$$p = \gamma kTn$$

so that when γ is set to zero, the dynamic pressure is also zero and the plasma is incompressible since the electrokinetic (EK) wave does not propagate. If instead, the plasma is of zero temperature, then the total pressure

is zero. The plasma may thus be of non-zero temperature and may or may not be compressible, but is always incompressible when the temperature is zero. In the results to follow, we assign a value of 3 to γ, so that $\gamma kT = mv_r^2$, with v_r the rms electron velocity. If we Fourier analyze the variables with respect to time appearing in (8) - (11) by using the transform pair

$$\underline{e}(\underline{r}, t) = \frac{1}{2\pi} \int_{-\infty}^{\infty} e^{i\omega t} \, \tilde{\underline{e}}(\underline{r}, \omega) \, d\omega$$

$$\tilde{\underline{e}}(\underline{r}, \omega) = \int_{-\infty}^{\infty} e^{-i\omega t} \, \underline{e}(\underline{r}, t) \, dt$$

then we obtain

$$\nabla \times \tilde{\underline{e}}(\underline{r}, \omega) = -i\omega\mu_o \tilde{\underline{h}}(\underline{r}, \omega) \tag{12}$$

$$\nabla \times \tilde{\underline{h}}(\underline{r}, \omega) = i\omega \epsilon_o \tilde{\underline{e}}(\underline{r}, \omega) - qN\tilde{\underline{v}}(\underline{r}, \omega) \tag{13}$$

$$i\omega U \tilde{\underline{v}}(\underline{r}, \omega) = -\frac{q}{m} \tilde{\underline{e}}(\underline{r}, \omega) - \frac{v_r^2}{N} \nabla \tilde{n}(\underline{r}, \omega) - \frac{q}{m} \mu_o H \tilde{\underline{v}}(\underline{r}, \omega) \times \hat{z} \tag{14}$$

$$i\omega \tilde{n}(\underline{r}, \omega) + N \cdot \tilde{\underline{v}}(\underline{r}, \omega) = 0 \tag{15}$$

where $U = 1 - i\nu/\omega = 1 - iZ$

After a further Fourier transform with respace to z, given by

$$\tilde{\underline{e}}(\underline{r}, \omega) = \frac{1}{2\pi} \int_{-\infty}^{\infty} e^{i\beta z} \, \tilde{\tilde{\underline{e}}}(\rho, \beta, \omega) \, d\beta$$

$$\tilde{\tilde{\underline{e}}}(\rho, \beta, \omega) = \int_{-\infty}^{\infty} e^{-i\beta z} \, \tilde{\underline{e}}(\underline{r}, \omega) \, dz$$

we can solve for the electron velocity from (13) - (15) to obtain

$$\approx\!\!\approx\!\!\sim \quad \tilde{v}_z = -\frac{q}{im\omega U}\,\tilde{e}_z - \frac{\beta v_r^2}{NU\omega}\,\tilde{n} \tag{16a}$$

$$\tilde{v}_\varphi = \frac{1}{qN(1-Y^2/U^2)}\left[\frac{i\omega_p^2\epsilon_o}{\omega U}\left(\tilde{e}_\varphi + \frac{Y}{iU}\,\tilde{e}_\rho\right) + \frac{qv_r^2 Y}{\omega U^2}\,\tilde{n}'\right] \tag{16b}$$

$$\tilde{v}_\rho = \frac{1}{qN(1-Y^2/U^2)}\left[\frac{i\omega_p^2\epsilon_o}{\omega U}\left(\tilde{e}_\rho - \frac{Y}{iU}\,\tilde{e}_\varphi\right) + \frac{iqv_r^2}{\omega U}\,\tilde{n}'\right] \tag{16c}$$

where the explicit dependence of the transformed quantities on β and ω is hereafter understood, and the prime denotes differentiation with respect to ρ. Note that the fact has been used that the field quantities are independent of the azimuthal coordinate φ, since the source is independent of φ. Also

$$\omega_p^2 = \frac{q^2 N}{\epsilon_o m}$$

$$\omega_h = \frac{qH\mu_o}{m}$$

$$X = \frac{\omega_p^2}{\omega^2}$$

$$Y = \frac{\omega_h}{\omega}$$

The velocity expressions may be inserted into (13) to get

$$\nabla \times \tilde{\underline{h}} = i\omega\epsilon_o(\underline{\epsilon}\cdot\tilde{\underline{e}} - \underline{k}\cdot\nabla\tilde{n}) \tag{13a}$$

where

$$\underline{\underline{\epsilon}} = \begin{bmatrix} \epsilon_1 & -\epsilon' & 0 \\ \epsilon' & \epsilon_1 & 0 \\ 0 & 0 & \epsilon_3 \end{bmatrix} \tag{17a}$$

$$\underline{\underline{k}} = \begin{bmatrix} k_1 & 0 & 0 \\ k' & 0 & 0 \\ 0 & 0 & k_3 \end{bmatrix} \tag{17b}$$

and

$$\epsilon_1 = 1 - \frac{XU}{U^2 - Y^2} \tag{17c}$$

$$\epsilon' = -i \frac{XY}{U^2 - Y^2} \tag{17d}$$

$$\epsilon_3 = 1 - \frac{X}{U} \tag{17e}$$

$$k_1 = \frac{qv_r{}^2 U}{\epsilon_o \omega^2 (U^2 - Y^2)} \tag{17f}$$

$$k' = -i \frac{qv_r{}^2 Y}{\epsilon_o \omega^2 (U^2 - Y^2)} \tag{17g}$$

$$k_3 = \frac{qv_r{}^2}{\epsilon_o \omega^2 U} \tag{17h}$$

Upon taking the curl of (12) and the curl and divergence of (13) together with the use of (15), we may obtain, after some simplification, the following coupled wave equations

$$\nabla_\rho^2 \tilde{\tilde{h}}_z + (K_{Eo}^2 \epsilon_3 - \beta^2)\tilde{\tilde{h}}_z + i\beta\epsilon_o \frac{XY\omega}{U^2}\tilde{\tilde{e}}_z + \frac{q\omega Y}{U}\left(1 - \frac{\beta^2 v_r^2}{\omega^2 U^2}\right)\tilde{\tilde{n}} = 0 \tag{18}$$

$$\nabla_\rho^2 \tilde{\tilde{e}}_z + (K_{Eo}^2 \epsilon_3 - \beta^2)\tilde{\tilde{e}}_z + \frac{i\beta q}{\epsilon_o}\left(1 - \frac{K_{Eo}^2 v_r^2}{\omega^2 U^2}\right)\tilde{\tilde{n}} = 0 \tag{19}$$

$$\nabla_\rho^2 \tilde{\tilde{n}} + \frac{q}{\epsilon_o k_1}\left(\epsilon_1 - \frac{\beta^2 v_r^2}{\omega^2 U^2}\right)\tilde{\tilde{n}} - \frac{i\beta\epsilon_o \omega^2 XY^2}{q v_r^2 U^2}\tilde{\tilde{e}}_z + \frac{i\omega\mu_o \epsilon'}{k_1}\tilde{\tilde{h}}_z = 0 \tag{20}$$

where $\nabla_\rho^2 = \frac{1}{\rho}\frac{\partial}{\partial\rho}\left(\rho\frac{\partial}{\partial\rho}\right)$, $K_{Eo}^2 = \omega^2\mu_o\epsilon_o$

It is of interest to see that $\tilde{\tilde{h}}_z$ appears in only two of the three wave equations. As a check, the system of equations (18) - (20) should reduce to the incompressible plasma equations given in II when $v_r \to 0$. Thus when the electron temperature becomes zero, (18) - (20) become

$$\nabla_\rho^2 \tilde{\tilde{h}}_z + (K_{Eo}^2 \epsilon_3 - \beta^2)\tilde{\tilde{h}}_z + i\beta\epsilon_o\omega \frac{XY}{U^2}\tilde{\tilde{e}}_z + q\omega\frac{Y}{U}\tilde{\tilde{n}} = 0 \tag{21}$$

$$\nabla_\rho^2 \tilde{\tilde{e}}_z + (K_{Eo}^2 \epsilon_3 - \beta^2)\tilde{\tilde{e}}_z + i\beta\frac{q}{\epsilon_o}\tilde{\tilde{n}} = 0 \tag{22}$$

$$\frac{q\epsilon_1}{\epsilon_o}\tilde{\tilde{n}} - i\frac{\beta XY^2}{U(U^2 - Y^2)}\tilde{\tilde{e}}_z + i\omega\mu_o\epsilon'\tilde{\tilde{h}}_z = 0 \tag{23}$$

It may be seen that $\tilde{\tilde{n}}$ is not zero unless Y = 0, a result also shown by (13) and (15) which yield

$$\epsilon_o \nabla\cdot\tilde{\tilde{\underline{e}}} + q\tilde{\tilde{n}} = 0$$

and since from (13a) we get

$$\nabla\cdot(\underline{\epsilon}\cdot\tilde{\tilde{\underline{e}}}) = 0$$

we then find

$$\nabla\cdot\tilde{\tilde{\underline{e}}} \neq 0$$

Equations (21) - (23) may be simplified to

$$\nabla_\rho^2 \tilde{\tilde{h}}_z + \left[K_{Eo}^2 \epsilon_1 \left(1 + \frac{\epsilon'^2}{\epsilon_1^2}\right) - \beta^2 \right] \tilde{\tilde{h}}_z - \beta \omega \epsilon_o \epsilon' \frac{\epsilon_3}{\epsilon_1} \tilde{\tilde{e}}_z = 0 \tag{24}$$

$$\nabla_\rho^2 \tilde{\tilde{e}}_z + \left[K_{Eo}^2 - \frac{\beta^2}{\epsilon_1} \right] \epsilon_3 \tilde{\tilde{e}}_z + \beta \omega \mu_o \frac{\epsilon'}{\epsilon_1} \tilde{\tilde{h}}_z = 0 \tag{25}$$

with the details shown in Appendix A. The expressions (24) and (25) are identical to the wave equations obtained in II for the anisotropic, incompressible plasma.

Returning now to the compressible plasma equations (18) - (20), we introduce

$$\begin{bmatrix} \tilde{\tilde{e}}_z \\ \tilde{\tilde{h}}_z \\ \tilde{\tilde{n}} \end{bmatrix} = \begin{bmatrix} & T & \end{bmatrix} \begin{bmatrix} G_1 \\ G_2 \\ G_3 \end{bmatrix} = \underline{\underline{T}} \cdot \underline{G} \tag{26}$$

so that

$$\left(\nabla_\rho^2 + \underline{\underline{C}} \cdot \right) \underline{\underline{T}} \cdot \underline{G} = 0 \tag{27}$$

where

$$\underline{\underline{C}} = \begin{bmatrix} K_{Eo}^2 \epsilon_3 - \beta^2 & ; & 0 & ; & i\beta\, q(1 - K_{Eo}^2 v_r^2/\omega^2 U)/\epsilon_o \\ i\beta \epsilon_o XY\omega/U^2 & ; & K_{Eo}^2 \epsilon_3 - \beta^2 & ; & q\omega Y(1 - \beta^2 v_r^2/\omega^2 U)/U \\ -i\beta \epsilon_o \omega^2 XY^2/q v_r^2 U^2 & ; & i\omega\mu_o \epsilon'/k_1 & ; & q(\epsilon_1 - \beta^2 v_r^2/\omega^2 U)/\epsilon_o k_1 \end{bmatrix} \tag{28}$$

Multiplying (27) from the left by T^{-1} we obtain

$$\left(\nabla_\rho^2 + \underline{\underline{T}}^{-1} \cdot \underline{\underline{C}} \cdot \underline{\underline{T}} \cdot \right) \underline{G} = 0 \tag{29}$$

A solution for the coupled plasma fields may be obtained if the matrix $\underline{\underline{T}}^{-1} \cdot \underline{\underline{C}} \cdot \underline{\underline{T}}$ can be diagonalized. If the columns of $\underline{\underline{T}}$ are the eigen vectors of $\underline{\underline{C}}$, defined by

$$\underline{\underline{C}} \cdot \underline{T}^{(j)} = \lambda_j T^{(j)} \tag{30a}$$

where $\underline{T}^j$ is the $j^{'}$th column of $\underline{\underline{T}}$ and λ_j is the corresponding eigen value, then

$$\underline{\underline{C}} \cdot \underline{\underline{T}} = \underline{\underline{C}} \cdot \left[\underline{T}^{(1)} + \underline{T}^{(2)} + \underline{T}^{(3)} \right] = \left[\lambda_1 \underline{T}^{(1)} + \lambda_2 \underline{T}^{(2)} + \lambda_3 \underline{T}^{(3)} \right]$$

Multiplying from the left by T^{-1} we get

$$\underline{\underline{T}}^{-1} \cdot \underline{\underline{C}} \cdot \underline{\underline{T}} = \underline{\underline{T}}^{-1} \cdot \left[\lambda_1 \underline{T}^{(1)} + \lambda_2 \underline{T}^{(2)} + \lambda_3 \underline{T}^{(3)} \right]$$

But

$$\underline{\underline{T}}^{-1} \cdot \underline{T}^{(1)} = \begin{bmatrix} 1 \\ 0 \\ 0 \end{bmatrix}$$

and similarly for $\underline{\underline{T}}^{-1} \cdot \underline{T}^{(2)}$ and $\underline{\underline{T}}^{-1} \cdot \underline{T}^{(3)}$ so that

$$\underline{\underline{T}}^{-1} \cdot \underline{\underline{C}} \cdot \underline{\underline{T}} = \underline{\underline{\lambda}} \tag{30b}$$

where

$$\underline{\underline{\lambda}} = \begin{bmatrix} \lambda_1 & 0 & 0 \\ 0 & \lambda_2 & 0 \\ 0 & 0 & \lambda_3 \end{bmatrix}$$

Solutions for the individual G's are thus

$$(\nabla_\rho^2 + \lambda_j)\, G_j = 0 \quad ; \quad j = 1, 2, 3 \tag{31}$$

and may be written, for the cylindrical geometry, as

$$G_j = A_j H_o^{(2)} (\sqrt{\lambda}_j \rho) \tag{32}$$

where $H_o^{(2)}$ is the Hankel function of the second kind and order zero, and the A_j's are the wave amplitudes to be determined by the boundary conditions. In order to ensure the proper behavior or the solutions at infinity, the roots of λ_j having a negative imaginary part must be used.

The eigen values of $\underline{\underline{C}}$ are solutions, with $\underline{\underline{I}}$ the identity matrix, to

$$\left| \underline{\underline{C}} - \lambda \underline{\underline{I}} \right| = 0$$

which is explicitly given by

$$\lambda^3 + a_2 \lambda^2 + a_1 \lambda + a_0 = 0$$

where

$$a_2 = -(C_{11} + C_{12} + C_{13})$$

$$a_1 = C_{11}C_{22} + C_{22}C_{33} + C_{33}C_{11} - C_{13}C_{31} - C_{23}C_{32}$$

$$a_0 = C_{13}C_{22}C_{31} + C_{11}C_{23}C_{32} - C_{32}C_{13}C_{21} - C_{11}C_{22}C_{33}$$

Finally, the eigen vectors $\underline{T}^j$ are obtained from (30a). Since there are nine homogeneous equations in the nine elements of $\underline{\underline{T}}$ represented by (30a) it is clear that a non-trival solution is possible only if some of the elements of $\underline{\underline{T}}$ are arbitrary. Since in addition, the nine equations break up into three sets of three unknowns, each set (j = 1, 2, 3) involving the three elements of each eigen vector $\underline{T}^j$, it is clear that three of the elements of $\underline{\underline{T}}$ are arbitrary. For convenience, we set the T_1^j elements equal to 1, so that

$$T_2^j = \left[(\lambda_j - C_{11})C_{23} + C_{13} + C_{21} \right] / \left[C_{13}(\lambda_j - C_{22}) \right]$$

$$T_3^j = (\lambda_j - C_{11}) / C_{13}$$

where j = 1, 2, 3

The quantities $\approx{e}_z$, $\approx{h}_z$ and $\approx{n}$ now serve as potentials from which the other field components may be found, as

$$\tilde{\tilde{De}}_\rho = C^+\tilde{\tilde{n}}' - i\beta\,\tilde{\tilde{Ae}}_z' - i\omega\mu_o\tilde{\tilde{Bh}}_z' \tag{33a}$$

$$\tilde{\tilde{De}}_\varphi = C^-\tilde{\tilde{n}}' + i\beta\,\tilde{\tilde{Be}}_z' - i\omega\mu_o\tilde{\tilde{Ah}}_z' \tag{33b}$$

$$\tilde{\tilde{Dh}}_\rho = D\beta\,\tilde{\tilde{e}}_\varphi/\omega\mu_o \tag{34a}$$

$$\tilde{\tilde{Dh}}_\varphi = \left[-i\beta\,C^+\tilde{\tilde{n}}' + (D-\beta^2 A)\,\tilde{\tilde{e}}_z' - \omega\mu_o\tilde{\tilde{Bh}}_z'\right]/i\omega\mu_o \tag{34b}$$

where

$$A = \beta^2 - K_{Eo}^2\,\epsilon_1$$

$$B = K_{Eo}^2\,\epsilon'$$

$$D = A^2 + B^2$$

$$C^+ = -K_{Eo}^2\,(Ak_1 + Bk')$$

$$C^- = -K_{Eo}^2\,(Ak' - Bk_1)$$

Now that the field quantities in the compressible magnetoplasma have been obtained in terms of the potentials $\tilde{\tilde{e}}_z$, $\tilde{\tilde{h}}_z$, and $\tilde{\tilde{n}}$, or equivalently in terms of the Gj, the boundary value problem for the vacuum sheath model can be specified. Seven scalar boundary condition equations are required for this purpose since there are three amplitude coefficients to be determined for the plasma fields, and four for the vacuum sheath where there are both inward and outward propagating transverse electric (TE) ($e_z = 0$) and transverse magnetic (TM) ($h_z = 0$) fields. The sheath fields may be generated in terms of potential functions also, where

$$\tilde{\tilde{\underline{e}}}_e = \nabla \times (\tilde{\tilde{\phi}}_e \hat{z}) \tag{35a}$$

$$\tilde{\tilde{\underline{e}}}_m = \frac{1}{K_{Eo}}\nabla\times\nabla\times(\tilde{\tilde{\phi}}_m \hat{z}) \tag{35b}$$

and $$\tilde{\tilde{\underline{h}}} = \frac{1}{-i\omega\mu_o}\nabla\times\tilde{\tilde{\underline{e}}}$$

The subscripts e and m refer respectively to the TE and TM fields, and upon using the superscripts I and R to denote the fields propagating in the $+\rho$ and $-\rho$ directions in the sheath, the potentials are of the form

$$\tilde{\tilde{\phi}}_{e,m}^{I,R} = A_{e,m}^{I,R} H_o^{(1,2)}(\lambda_{Eo}\rho) \tag{36}$$

with $\lambda_{Eo}^2 = K_{Eo}^2 - \beta^2$

We use the usual boundary conditions of continuity of the tangential electric and magnetic fields at the vacuum sheath-uniform plasma interface (ρ=s) and vanishing of $\tilde{\tilde{e}}_\phi$ on the surface of the perfectly conducting antenna (ρ=c), which is a total of five scalar boundary condition equations. The final two equations involve the field at the exciting circumferential gap on the antenna surface, and the normal electron velocity at the sheath-plasma interface. A voltage $e^{i\omega' t}$ excites the antenna, being applied across a circumferential gap of thickness δ centered at z = 0. The axial electric field vanishes everywhere on the antenna surface except at the gap where it is assumed equal to the gap field, which for δ small compared with the excited wave-lengths, is given by $-e^{i\omega' t}/\delta$. Thus

$$\tilde{\tilde{e}}_z(c,\beta,\omega) = -\delta(\omega-\omega')\, 2\pi \frac{\sin(\beta\delta/2)}{(\beta\delta/2)} \tag{37}$$

$$= +2\pi\delta(\omega-\omega')\, S(\beta)$$

The boundary condition on the electron velocity at the sheath-plasma interface, is written as, for the sake of generality,

$$\tilde{\tilde{v}}_\rho = Y_B \tilde{\tilde{n}} \tag{38}$$

where Y_B is the surface admittance (Cohen, 1962), and may be non-zero for an absorptive - type boundary (Balmain, 1966).

The seven scalar boundary condition equations are then written

$$\frac{\lambda_{Eo}^2}{K_{Eo}} (A_m^I H_{c2} + A_m^R H_{c1}) = S(\beta)\, 2\pi \delta(\omega-\omega') \tag{39}$$

$$A_e^I H'_{c2} + A_e^R H'_{c1} = 0 \tag{40}$$

$$\frac{\lambda_{Eo}^2}{K_{Eo}} (A_m^I H_{s2} + A_m^R H_{s1}) = \tilde{\tilde{e}}_z(s,\beta,\omega) \tag{41}$$

$$-\lambda_{Eo} (A_e^I H'_{s2} + A_e^R H'_{s1}) = \tilde{\tilde{e}}_\varphi(s,\beta,\omega) \tag{42}$$

$$\frac{i\lambda_{Ec}^2}{\eta_o K_{Eo}} (A_e^I H_{s2} + A_e^R H_{s1}) = \tilde{\tilde{h}}_z(s,\beta,\omega) \tag{43}$$

$$\frac{-i\lambda_{Eo}}{\eta_o} (A_m^I H'_{s2} + A_m^R H'_{s1}) = \tilde{\tilde{h}}_\varphi(s,\beta,\omega) \tag{44}$$

$$\frac{U^2}{(U^2-Y^2)}\left[\frac{iX\epsilon_o\omega}{U}(\tilde{\tilde{e}}_\rho(s,\beta,\omega) - \frac{Y}{iU}\tilde{\tilde{e}}(s,\beta,\omega)\right. \tag{45}$$

$$\left. + \frac{iqv_r^2}{\omega U}\frac{d}{d\rho}\tilde{\tilde{n}}(\rho,\beta,\omega)\right|_{\rho=s} = Y_B\tilde{\tilde{n}}(s,\beta,\omega)$$

where

$$H_{Xn} = H_o^{(n)}(\lambda_{Eo}X),$$

the prime denotes differentiation with respect to argument, and

$$\eta_o = \sqrt{\mu_o/\epsilon_o}\ .$$

The system of equations (39) - (45) is quite complicated, particularly when the dependence of the various plasma fields upon the Gj solutions is considered. Some simplification can be effected by using (39) and (40) to eliminate two of the coefficients, thus leaving five equations in five unknowns to be solved. The extreme complexity of solving this system of equations indicated the utility, for now at least, of attacking the sheathless case instead. This has the advantage of providing a check solution for a possible subsequent numerical treatment of the vacuum sheath problem, while at the same time being sufficiently less involved as to be numerically feasible to treat.

II. 2. The Sheathless Case.

When there is no sheath (or equivalently for the vacuum sheath case, when s = c), then the nine boundry condition equations (39) to (45) simplify to

$$\tilde{\tilde{e}}_z(c,\beta,\omega) = S(\beta)\, 2\pi\delta(\omega-\omega') \tag{46}$$

$$\tilde{\tilde{e}}_\phi(c,\beta,\omega) = 0 \tag{47}$$

$$\frac{i}{qN}\left[\omega\epsilon_o\tilde{\tilde{e}}_\rho(c,\beta,\omega)+\beta\tilde{\tilde{h}}_\phi(c,\beta,\omega)\right] = Y_B\tilde{\tilde{n}}(c,\beta,\omega) \tag{48}$$

In the calculations to follow, we take $Y_B = 0$ (i.e., the rigidity boundary condition) so that in the following development the right hand side of (48) is set equal to zero. The substitution of the potentials $\tilde{\tilde{e}}_z$, $\tilde{\tilde{h}}_z$ and $\tilde{\tilde{n}}$ into (47) and (48) leads to, with the prime denoting differentiation with respect to ρ,

$$C^-\tilde{\tilde{n}}' + i\beta B\tilde{\tilde{e}}_z' - i\omega\mu_o A\tilde{\tilde{h}}_z' = 0 \tag{49}$$

$$-C^+\tilde{\tilde{n}}' + i\beta\left[A-D/(\beta^2-K_{Eo}^2)\right]\tilde{\tilde{e}}_z' + i\omega\mu_o B\tilde{\tilde{h}}_z' = 0 \tag{50}$$

where the potentials are understood to functions of ρ,β and ω evaluated at $\rho=c$. It is convenient to eliminate $\tilde{\tilde{n}}'$ and $\tilde{\tilde{h}}_z'$ from one of the two equations in which they appear, so that (49) and (50) become

$$F_1\tilde{\tilde{h}}_z' + F_2\tilde{\tilde{e}}_z' = 0 \tag{51}$$

$$F_1\tilde{\tilde{n}}' + F_3\tilde{\tilde{e}}_z' = 0 \tag{52}$$

where

$$F_1 = i\omega\mu_o(BC^- - AC^+)$$

$$F_2 = i\beta\left[BC^+ + C^-\left[A-D/(\beta^2-K_{Eo}^2)\right]\right]$$

$$F_3 = -\omega\mu_o\beta\left[B^2 + A\left[A-D/(\beta^2-K_{Eo}^2)\right]\right]$$

which together with (46), (26) and (32) serve to obtain the A_j wave amplitudes.

Upon introducing the following notation

$$H_{ij}' = T_{ij} H_o^{(2)'}(\sqrt{\lambda}_j c)$$

$$H_{ij} = T_{ij} H_o^{(2)}(\sqrt{\lambda}_j c)$$

the boundary condition equations may be written

$$(F_1 H_{21}' + F_2 H_{11}') A_1 + (F_1 H_{22}' + F_2 H_{12}') A_2 + (F_1 H_{23}' + F_2 H_{13}') A_3 = 0 \quad (53)$$

$$(F_1 H_{31}' + F_3 H_{11}') A_1 + (F_1 H_{32}' + F_3 H_{12}') A_2 + (F_1 H_{33}' + F_3 H_{13}') A_3 = 0 \quad (54)$$

$$H_{11} A_1 + H_{12} A_2 + H_{13} A_3 = S(\beta)\, 2\pi \delta(\omega - \omega') \quad (55)$$

There does not appear to be any advantage in analytically inverting the Eqns. (53) to (55) because of the complexity of the coefficients; the inversion was consequently done numerically. The φ-component of magnetic field, required to obtain the axial antenna current, is then obtained as

$$\tilde{\tilde{h}}_{\varphi}(c,\beta,\omega) = \frac{1}{i\omega\mu_o D}\left[C_1 A_1 + C_2 A_2 + C_3 A_3\right] \quad (56)$$

where

$$C_j = (D - \beta^2 A) H_{1j}' - \beta\omega\mu_o B H_{2j}' - i\beta C^{+} H_{3j}'$$

while the z-component is given by

$$\tilde{\tilde{h}}_z(c,\beta,\omega) = H_{21} A_1 + H_{22} A_2 + H_{23} A_3 \quad (57)$$

The antenna surface current in the z-direction is obtained from

$$I_z(z,t) = h_\varphi(c,z,t)\, 2\pi c$$

$$= \frac{c}{2\pi}\int_{-\infty}^{\infty} e^{i(\omega' t + z)}\,\tilde{\tilde{h}}_\varphi(c,\beta,\omega')\, d\beta\, d\omega'$$

$$= 2ce^{i\omega t}\int_{-o}^{\infty} \cos(\beta z)\,\bar{h}_\varphi(c,\beta,\omega)\, d\beta$$

$$= I_z(z,\omega)\, e^{i\omega t} \qquad (58)$$

Similarly, we obtain the surface current in the azimuthal direction as

$$I_\varphi(z,t) = 2\pi c K_\varphi(c,z,t)$$

$$= -2\pi c h_z(c,z,t)$$

$$= -\frac{c}{2\pi}\iint_{-\infty}^{\infty} e^{i(\omega' t + \beta z)}\,\tilde{\tilde{h}}_z(c,\beta,\omega')\, d\beta\, d\omega'$$

$$= -2ce^{i\omega t}\int_{-o}^{\infty} \cos(\beta z)\,\bar{h}_z(c,\beta,\omega)\, d\beta$$

$$= I_\varphi(z,\omega)\, e^{i\omega t} \qquad (59)$$

where for purposes of comparison with I_z, we have multiplied the φ-directed surface current per unit length by $2\pi c$. Also

$$\tilde{\tilde{h}}_z(c,\beta,\omega') = 2\pi\,\delta(\omega-\omega')\,\bar{h}_z(c,\beta,\omega)$$

$$\tilde{\tilde{h}}_\varphi(c,\beta,\omega') = 2\pi\,\delta(\omega-\omega')\,\bar{h}_\varphi(c,\beta,\omega)$$

The antenna admittance Y, is for unit excitation voltage given by

$$I_z(\delta/2, \omega) = Y(\omega) = G(\omega) + iB(\omega) \tag{60}$$

and is obtained by a numerical integration of (58). A discussion of the numerical integration technique used is given in I. The accuracy of the admittance results to be presented should be better than one percent, unless otherwise indicated. Limitations on the accuracy are due principally to replacing the integration in (58) by a summation and truncating the integration at a finite value of β. The error associated with the former may be adjusted by specifying the convergence accuracy of the numerical integration, while the latter error is adjusted by specifying the allowable truncation error as discussed in I. An earlier termination of the integration then desired may sometimes result from computer overflow in which case the specified smallness of truncation error may not be achieved.

The evaluation of the admittance values for the present case of the compressible magnetoplasma was considerably more time consuming than required to obtain the results given in I and II primarily because finding the eigen values of the wave equations requires obtaining the complex zeros of a complex cubic equation. A typical admittance value for I and II required about one minute of 7090 time for its calculation, whereas in the present case, this time may be on the order of 3 or 4 minutes. The convergence test was used in evaluating the antenna admittance, or $I_z(\delta/2, \omega)$, so that as mentioned in II, the values obtained for $I_\varphi(\delta/2, \omega)$ may not be as accurate as those given for $I_z(\delta/2, \omega)$.

II. 3. The Inhomogeneous Sheath

For purposes of completeness, the equations requiring solution for the inhomogeneous sheath model are included here, though no numerical computations are included in this report for the inhomogeneous sheath. When the inhomogeneous sheath is considered, then the linearized variables introduced in (7) are modified by

$$\underline{E}(\underline{r}, t) = \underline{E}(\underline{r}) + \underline{e}(\underline{r}, t) \; ; \; |e| << |E| \tag{7a}'$$

$$N(\underline{r}, t) = N(\underline{r}) + n(\underline{r}, t) \; ; \; |n| << |N| \tag{7d}'$$

$$P(\underline{r}, t) = P(\underline{r}) + p(\underline{r}, t) \; ; \; |p| << |P| \tag{7e}'$$

so that in place of (10) we obtain

$$\frac{\partial}{\partial t}\underline{v}(\underline{r}, t) = -\frac{q}{m}\underline{e}(\underline{r}, t) - \nu\, \underline{v}(\underline{r}, t) + \frac{n(\underline{r}, t)}{mN^2(\underline{r})} \nabla P(\underline{r})$$

$$\frac{-1}{mN(\underline{r})} \nabla P(\underline{r}, t) - \frac{q}{m} \mu_o \underline{v}(\underline{r}, t) \times H\hat{z} \tag{10}'$$

while (11) is now

$$\frac{\partial}{\partial t} n(\underline{r}, t) + N(\underline{r}) \nabla \cdot \underline{v}(\underline{r}, t) + \underline{v}(\underline{r}, t) \cdot \nabla N(\underline{r}) = 0 \tag{11}'$$

We note that (10)' can be also written as

$$\frac{\partial}{\partial t}\underline{v}(\underline{r}, t) = -\frac{q}{m}\underline{e}(\underline{r}, t) - \nu\, \underline{v}(\underline{r}, t) - \frac{kT}{m} n(\underline{r}, t) \nabla N(\underline{r})^{-1} - \frac{\gamma kT}{mN(\underline{r})} \nabla n(\underline{r}, t)$$

$$- \frac{q}{m} \mu_o \underline{v}(\underline{r}, t) \times Hz$$

which more clearly demonstrates the result of a non-zero temperature or non-zero γ on the electron equation of motion.

It may be shown that using (10)' and (11)' in (9) leads to (13a) in the same way as before, but where now

$$\underline{\underline{k}} = \begin{bmatrix} k_1 & 0 & k_2 \\ k' & 0 & k_2' \\ 0 & 0 & k_3 \end{bmatrix}$$

and where

$$k_2 = \frac{-iXUkT}{q\beta(U^2-Y^2)} \nabla N(\underline{r})^{-1} = \frac{-iXE(\underline{r})U}{\beta N(\underline{r})(U^2-Y^2)}$$

$$k_2' = -i\frac{Y}{U}k_2$$

Thus the effect of the inhomogeneity is to introduce two additional terms in the $\underline{\underline{k}}$ matrix.

We find from (3) that

$$\frac{q}{m}E(\underline{r}) = -\frac{\nabla P(\underline{r})}{mN(\underline{r})} = -\frac{kT\nabla N(\underline{r})}{mN(\underline{r})} = -\frac{kT}{m}\frac{\partial}{\partial\rho}\ln N(\rho) \qquad (61a)$$

since N is a function of ρ only so that with

$$E(\rho) = -\nabla\phi(\rho) \qquad (61b)$$

we find

$$N(\rho) = N_\infty \exp(q\phi(\rho)/kT) \qquad (61c)$$

with N_∞ the electron density in the uniform plasma. We will assume that $\phi(r)$ varies as

$$\phi(\rho) = \phi_c\left[\frac{s-\rho}{s-c}\right]^M \quad ; \; c \leq \rho \leq s \qquad (61d)$$

where M is an adjustable parameter and

$$\phi_c = -\frac{kT}{q}\log_e\left[\sqrt{\frac{m_i}{m}}\frac{1}{1.22}\right] \qquad (61f)$$

with m_i the ion mass (see Self; 1963). It should be noted that these equations for the static sheath electric field and electron density are approximations at best for even the magnetic-field-free case. However, they seem to be a reasonable first order attempt to include the sheath inhomogeneity in the analysis.

It may be seen in (61) that $N(\rho)$ is independent of T, at least explicitly and could apparently be an arbitrary function of ρ, but since in reality the sheath thickness is proportional to the electron Debye length D_ℓ, where

$$D_\ell = v_r/(\sqrt{3}\omega_p) = \sqrt{kT/m}\,/\omega_p$$
$$= \sqrt{\epsilon_o kT/N_\infty q^2}$$

then $s \to c$ as $T \to 0$ so that the electron density variation would be confined to a decreasingly thinner region with decreasing temperature. Thus in considering either the vacuum sheath or inhomogeneous sheath models, a realistic sheath thickness presupposes consideration of a realistic electron temperature regardless of whether or not the compressible plasma model is being considered.

Since the first order differential equations are more convenient to deal with in a numerical analysis, we present here the first order differential equations which apply in the sheath. They are

$$\tilde{\tilde{e}}_z' = i\beta\tilde{\tilde{e}}_\rho + i\omega\mu_o\tilde{\tilde{h}}_\varphi \tag{62a}$$

$$\tilde{\tilde{e}}_\varphi' = -\frac{1}{\rho}\tilde{\tilde{e}}_\varphi - i\omega\mu_o\tilde{\tilde{h}}_z \tag{62b}$$

$$\tilde{\tilde{e}}_\rho' = -\frac{1}{\rho}\tilde{\tilde{e}}_\rho - i\beta\,\tilde{\tilde{e}}_z + \frac{i\omega'}{\epsilon_o v_r^2}\,\tilde{\tilde{Q}} \tag{62c}$$

$$\tilde{\tilde{h}}_\varphi' = i\omega\,\epsilon_o\epsilon_3\tilde{\tilde{e}}_z - i\beta\,\tilde{\tilde{Q}} - \frac{1}{\rho}\tilde{\tilde{h}}_\varphi \tag{62d}$$

$$\tilde{\tilde{h}}_z' = -\omega\,\epsilon_o\frac{Y}{U}\tilde{\tilde{e}}_\rho - i\omega\,\epsilon_o\epsilon_3\tilde{\tilde{e}}_\varphi + \beta\,\frac{Y}{U}\,\tilde{\tilde{h}}_\varphi + \frac{i\beta^2}{\omega\mu_o}\tilde{\tilde{e}}_\varphi \tag{62e}$$

$$\tilde{\tilde{Q}}' = -\frac{\epsilon_o\omega(U^2-Y^2)}{iU^2}\,\epsilon_1\tilde{\tilde{e}}_\rho + \epsilon_o\omega X\frac{Y}{U^2}\,\tilde{\tilde{e}}_\varphi\;\frac{-qE}{m v_r^2}\,\tilde{\tilde{Q}} \tag{62f}$$

$$+ i\beta\left(\frac{U^2-Y^2}{U^2}\right)\tilde{\tilde{h}}_\varphi$$

where

$$\tilde{\tilde{Q}} = -q v_r^2\tilde{\tilde{n}}/i\omega' = -q\,\gamma\,kT\tilde{\tilde{n}}/i\omega'\,m$$

These equations (62) reduce to those given in II for the inhomogeneous incompressible plasma by setting γ and E equal to zero. It is necessary to set E equal to zero in the dynamic equations given here to recover those in II since the equations in II were obtained by dropping at the outset the pressure term in the dynamic electron equation of motion, with the result that no term in $E\tilde{\tilde{Q}}$ arises in II, as does appear here in (62f). This occurs since in II the plasma is considered of zero temperature in the dynamic equations, but of non-zero temperature in the static equations in order to provide an inhomogeneous electron density distribution in the sheath. If the plasma is incompressible (i.e., $\gamma = 0$) but of non-zero temperature, then (62f) reduces to a linear relationship among $\tilde{\tilde{e}}_\rho$, $\tilde{\tilde{e}}_\varphi$, $\tilde{\tilde{h}}_\varphi$ and $\tilde{\tilde{Q}}$ and (61) represents a fifth-order differential equation. When in addition, E is set to zero in (62f) the results of II are then obtained. Finally, when Y is zero, the Equations (62) reduce to those for the inhomogeneous sheath of I.

The boundary value problems for the inhomogeneous sheath may be formulated in a fashion similar to that of I and II. The tangential electric and magnetic fields, the normal electron velocity and the electron number density are required to be continuous at the sheath-uniform plasma interface, yielding six scalar boundary conditions, where the fields in the uniform plasma are solutions to (21) to (23). The boundary conditions at the antenna surface are the same as those used for the sheathless case above, given by (46) to (48), in which the field quantities are now solutions to (62) to obtain a total of nine scalar equations. The Fourier coefficients for the transmitted fields in the uniform plasma may be eliminated from the boundary condition equations at the sheath uniform plasma interface as before, to obtain six scalar equations which determine the six constants of integration of (62a) to (62f).

III. Numerical Results

Because of the complexity of the boundary value problem for the infinite antenna in a compressible magnetoplasma, the previous discussion has been restricted, at least so far as any detail is concerned, to the sheathless case. Consequently, the numerical results to be presented here are also limited to the sheathless case. The plasma and antenna parameter values used in obtaining the results to follow have been chosed to conform to the corresponding values employed for the previous calculations presented in I and II .

For the purpose of comparison and to demonstrate the change from the free-space antenna admittance brought about by the immersion of the antenna in the plasma, Fig. 1 shows the free-space antenna conductance G_o and susceptance B_o as a function of frequency over the range 250 KHz to 10 MHz, with the exciting gap thickness δ a parameter, ranging from 10^{-1} to 10^{-3} cm and an antenna radius c of 1 cm. It may be seen in Fig. 1 that the free space conductance is independent of the exciting gap thickness and the susceptance is only slightly dependent upon the gap thickness, a feature discussed previously in more detail in I. In addition, over the frequency range used, the conductance exceeds the susceptance by a factor of about 5. In the subsequent graphs, the antenna radius will be 1 cm and the gap thickness 0.1 cm.

We now present in Fig. 2 the admittance when the antenna is immersed in the compressible, magnetoplasma medium with f_p = 1.5 MHz, f_h = 1.0 MHz, $\nu = 10^4 \text{sec}^{-1}$, T=1,500°K, $\delta = 10^{-1}$cm and c=1 cm. The vacuum sheath thickness, in units of the electron Debye length D_ℓ, is denoted by X on these and subsequent graphs; because this is the sheathless case, X=0. Above the upper hybrid frequency $f_t = \sqrt{f_p^2 + f_h^2}$, the conductance and susceptance are seen in Fig. 2 to be in approximately their free space ratios and increasing toward their free space values as the frequency is increased. There is a conductance

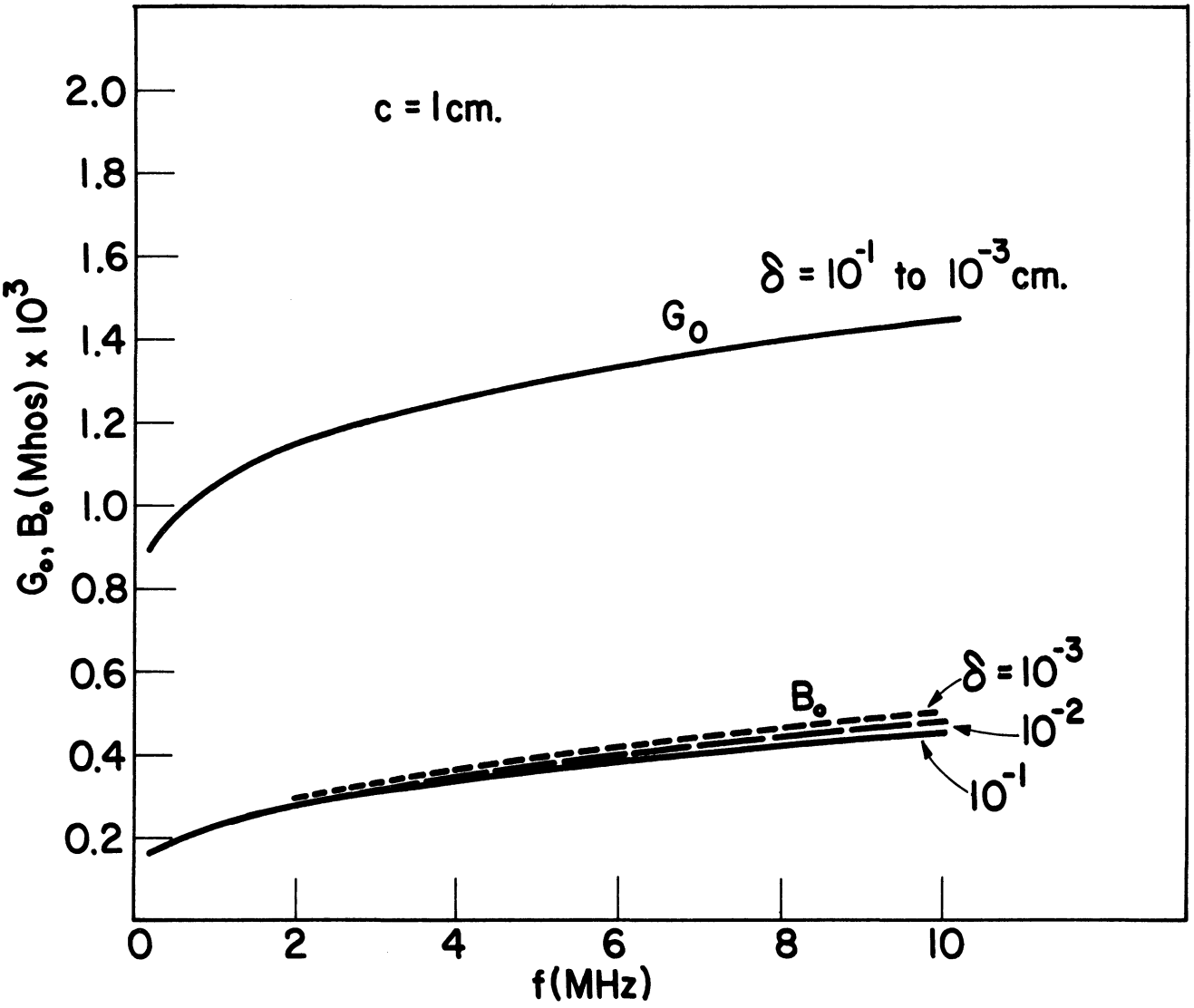

Figure 1. The free-space infinite cylindrical antenna admittance as a function of frequency with the exciting gap thickness, δ, a parameter and a radius, c, of 1 cm.

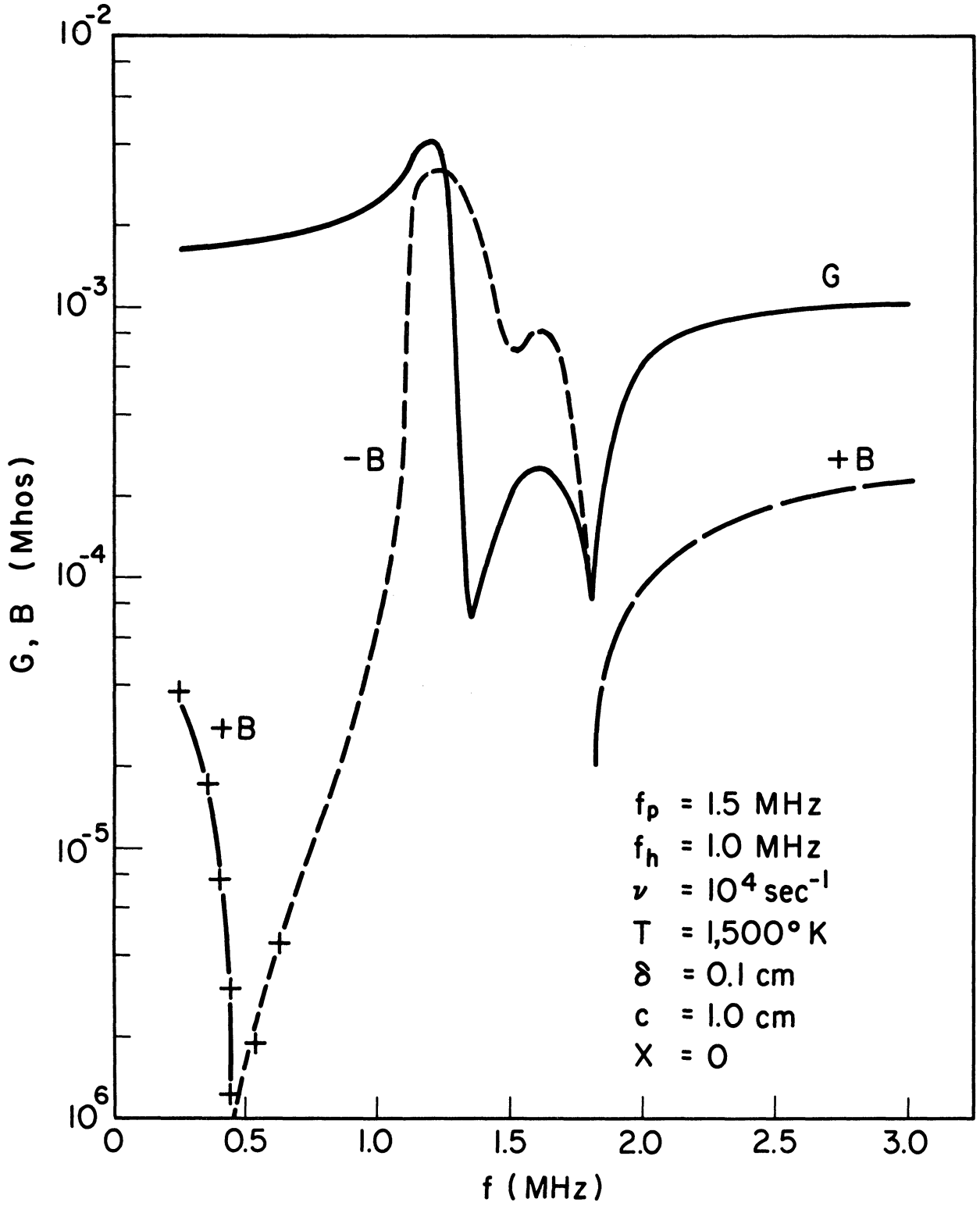

Figure 2. The infinite antenna admittance as a function of frequency for the compressible, magnetoplasma and the sheathless case with a radius of 1 cm, an electron plasma frequency of 1.5 MHz and electron cyclotron frequency of 1.0 MHz.

minimum and susceptance zero at $f = f_t$, the susceptance changing from capacitive above f_t to inductive immediately below it. As the frequency is decreased below f_t, a susceptance minimum or "kink" occurs at f_p, while the conductance has a rather sharp minimum just below f_p. A rather broad susceptance maximum occurs between f_p and f_h, where a somewhat sharper conductance maximum also is seen. Further decreasing the frequency below f_h results in a slowly decreasing conductance, and another susceptance zero, below which the susceptance is again capacitive. The low frequency part of the susceptance curve is marked with superimposed crosses since the susceptance values obtained here are estimated to be accurate to no better than 10 per cent; this coding will be used on subsequent graphs for the same purpose.

In Fig. 3 the infinite antenna admittance results are presented for the same set of parameter values as used for Fig. 2 with the exception that the values of f_p and f_h have been interchanged, f_p now being 1.0 MHz and f_h 1.5 MHz. The admittance above the hybrid frequency is similar to that for the previous case, there again being a conductance minimum and susceptance zero at f_t. As the frequency is decreased below f_t, the susceptance and conductance both exhibit maxima between f_t and f_h, with the conductance maximum occurring closer to f_t than the wider susceptance maximum. The susceptance again passes through zero close to f_h, below which it is capacitive. Another conductance minimum or kink is observed at f_p and a susceptance minimum is seen below f_p in a fashion similar to the results of Fig. 2 near f_p except that the roles of the conductance and susceptance are interchanged in the two graphs. The conductance for f sufficiently less than f_p is nearly independent of frequency.

The significance of the admittance curves shown in Figs. 2 and 3 can perhaps be more fully appreciated when compared with some of the admittance results of I and II. Therefore, for ease in comparing these results, we

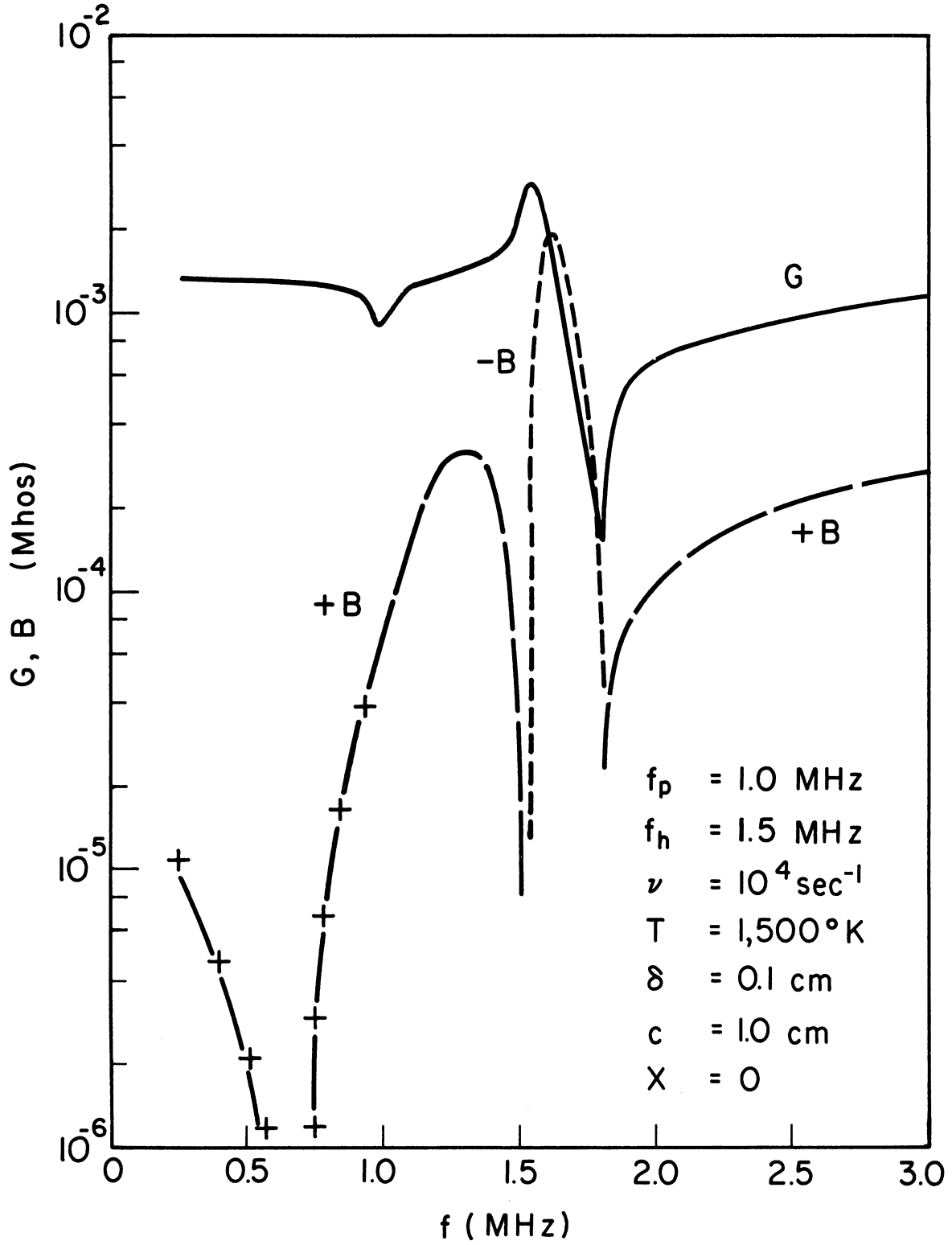

Figure 3. The infinite antenna admittance as a function of frequency for the compressible, magnetoplasma and the sheathless case with a radius of 1 cm, an electron plasma frequency of 1.0 MHz and electron cyclotron frequency of 1.5 MHz.

present in Figs. 4 and 5 the results corresponding to Figs. 2 and 3 respectively for the sheathless case, but for the incompressible plasma. The most obvious difference between the compressible magnetoplasma and incompressible magnetoplasma admittances is the fact that in the latter case, there is a very pronounced admittance maximum at f_h, while in the former case the admittance maximum is reduced in amplitude and shifted upward in frequency from f_h. In other aspects, the incompressible and compressible magnetoplasma admittance curves resemble each other, having other admittance maxima and minima of very similar nature.

It is very interesting to observe that when compared with the incompressible, sheathless magnetoplasma admittance results shown in Figs. 4 and 5, the additional effect on the admittance of the magnetoplasma compressibility shown in Figs. 2 and 3 is very similar to that resulting when the incompressible magnetoplasma is separated from the antenna by a vacuum sheath, the results for which are shown in Figs. 6 and 7. The sheath thickness used here is $5\,D_\ell$ calculated for an electron temperature of $1,500^{\circ}K$. A comparison of the admittance curves for the three cases considered shows that the vacuum sheath also shifts upward in frequency and reduces in amplitude the admittance maximum which occurs at f_h for the incompressible sheathless case, as was discussed above in presenting results for the compressible magnetoplasma model. Outside of this main difference, the admittance results for the three models are quite similar. It is thus apparent that at least from the viewpoint of the infinite antenna admittance, the magnetoplasma compressibility and vacuum sheath are factors, which taken separately, produce changes from the antenna admittance for the sheathless, incompressible case of very similar character.

This equivalence of the plasma compressibility and the vacuum sheath may be further illustrated by presenting comparable results for the isotropic (magnetic-field-free) plasma, as shown in Fig. 8 and 9. The results

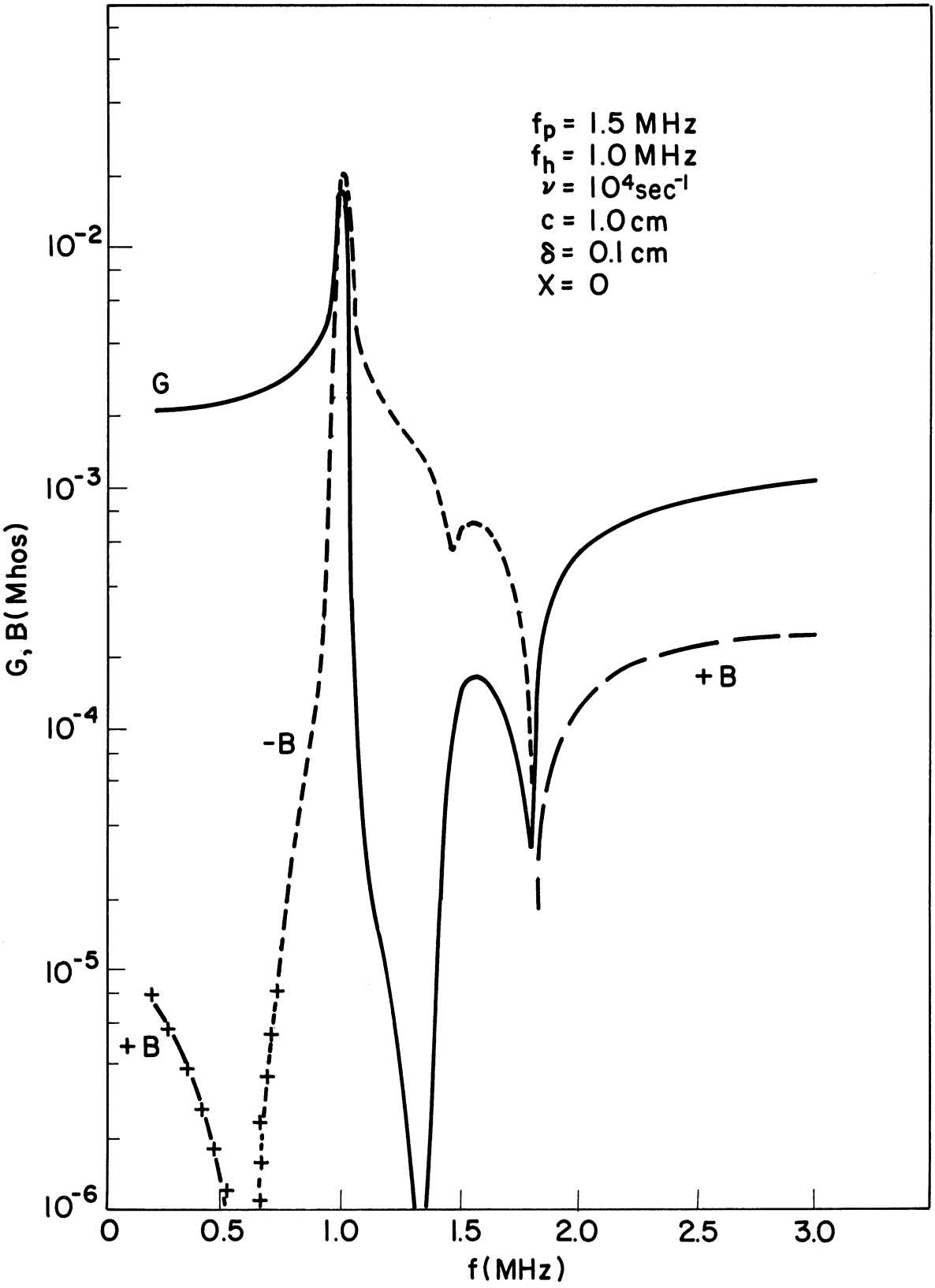

Figure 4. The infinite antenna admittance as a function of frequency for the incompressible magnetoplasma and the sheathless case, with an electron plasma frequency of 1.5 MHz and electron cyclotron frequency of 1.0 MHz.

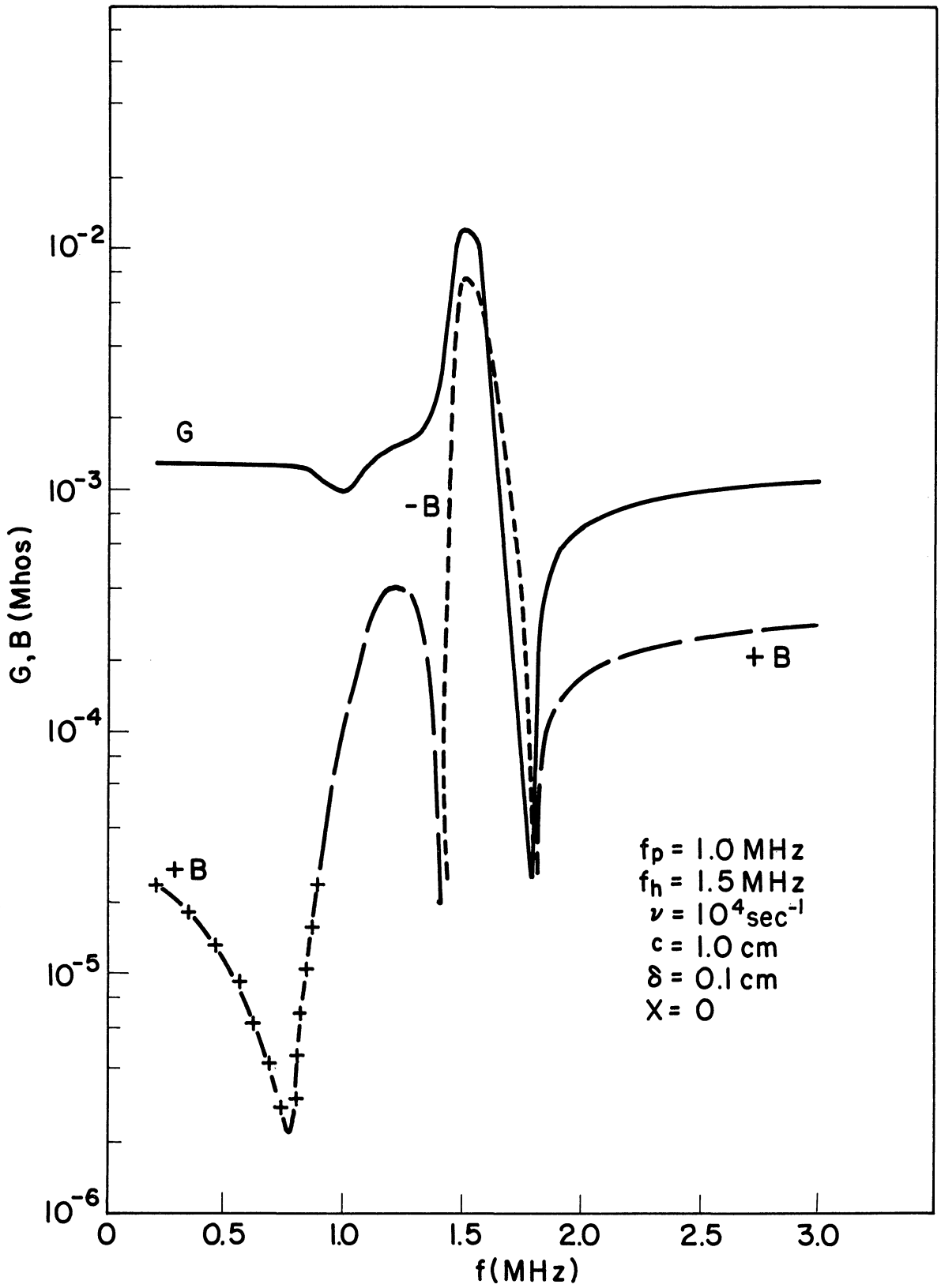

Figure 5. The infinite antenna admittance as a function of frequency for the incompressible magnetoplasma and the sheathless case, with an electron plasma frequency of 1.0 MHz and electron cyclotron frequency of 1.5 MHz.

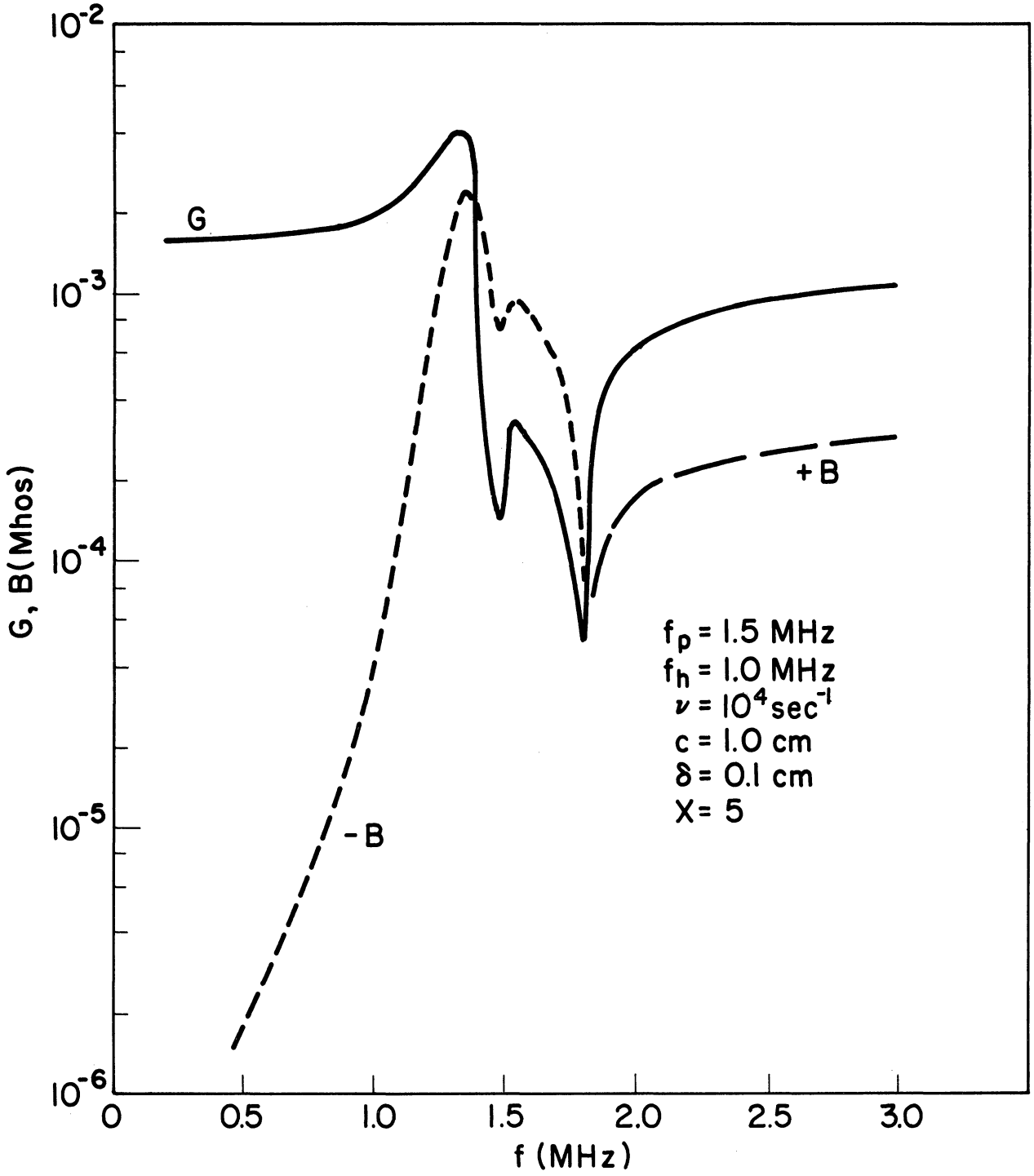

Figure 6. The infinite antenna admittance as a function of frequency in the incompressible magnetoplasma with a vacuum sheath thickness of 5 D_ℓ, an electron plasma frequency of 1.5 MHz and electron cyclotron frequency of 1.0 MHz.

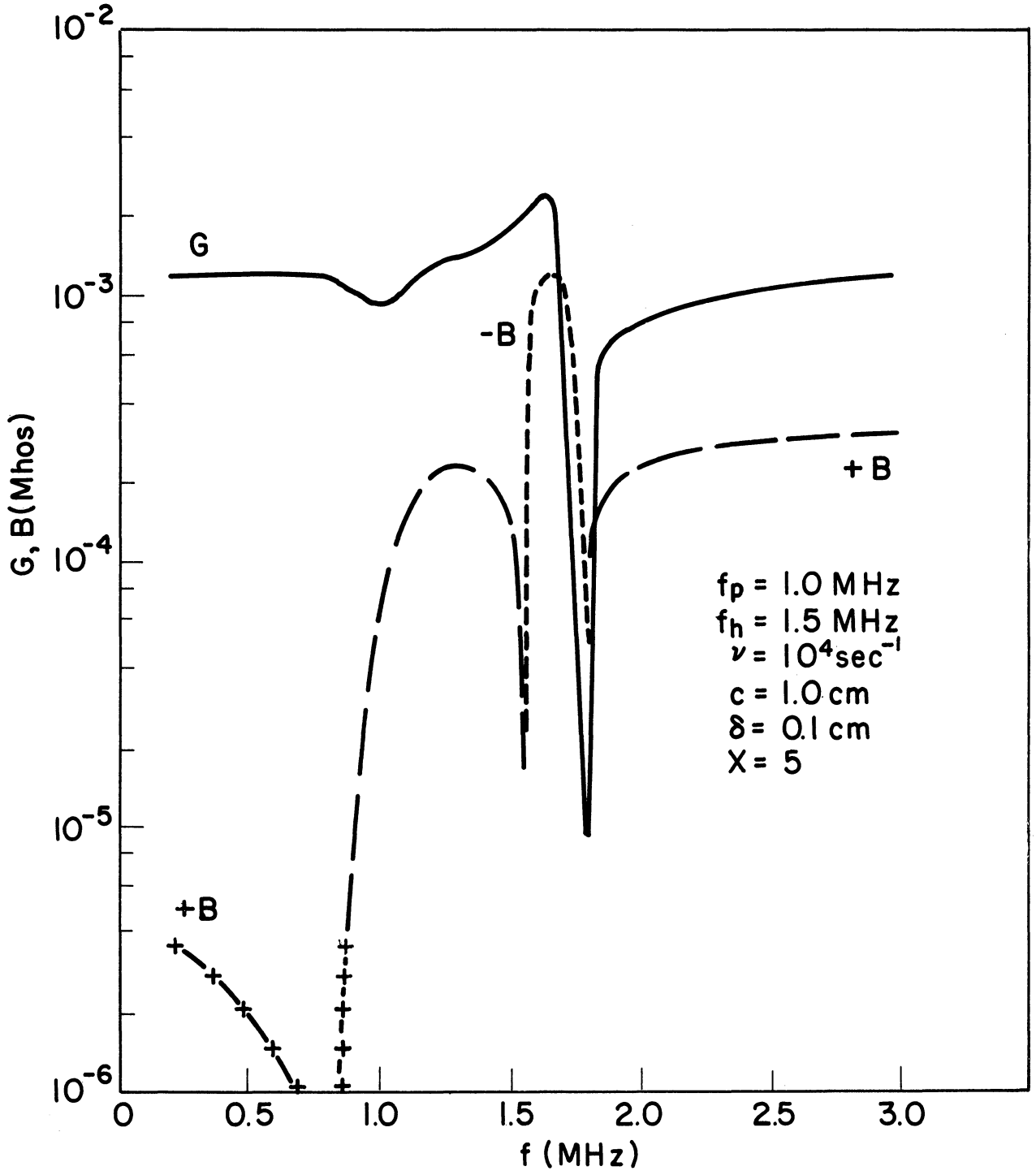

Figure 7. The infinite antenna admittance as a function of frequency in the incompressible magnetoplasma with a vacuum sheath thickness of 5 $D\ell$, an electron plasma frequency of 1.0 MHz and electron cyclotron frequency of 1.5 MHz.

of Fig. 8 are for the sheathless case and those of Fig. 9 are for the 5 D_ℓ vacuum sheath (the electron temperature used for calculating the sheath thickness is again 1,500°K) with f_p equal to 1.5 MHz. The incompressible plasma curves are denoted by T=0°K. It may be seen in Figs. 8 and 9 that as for the magnetoplasma case, the plasma compressibility and vacuum sheath, taken separately, change the admittance from the sheathless, incompressible case in very similar fashion. In particular, an admittance maximum occurs below the plasma frequency (at roughly half the plasma frequency for the cases shown) whenever there is a sheath or the plasma is compressible. Thus we wee that in the isotropic plasma, as for the anisotropic case discussed above, a similar influence is exercised by the plasma compressibility and vacuum sheath on the infinite antenna admittance. Consequently, while admittance results are not given here for the compressible, sheathed, magnetoplasma case, it appears, based on the results thus far shown, that this model would not be expected to be very significantly different from the sheathless case already considered. Part of the explanation of the antenna admittance on the plasma anisotropy, plasma compressibility and the vacuum sheath comes from the nature of the current waves excited on the infinite antenna for these various plasma models. This topic is of sufficient interest and depth to justify a separate discussion, to be given in a subsequent report.

Although not as significant a physical quantity as the axial antenna current, the circumferential current has some significance, since it is determined by the TE mode axial magnetic field, which is of course zero when the plasma is isotropic. It may thus be viewed as an indicator of the magnetoplasma anisotropy as seen by the antenna, when compared with the axial current, which comes from the TM mode circumferential magnetic field; the magnitudes, of the two currents serve to indicate the degree of excitation of the two electromagnetic modes.

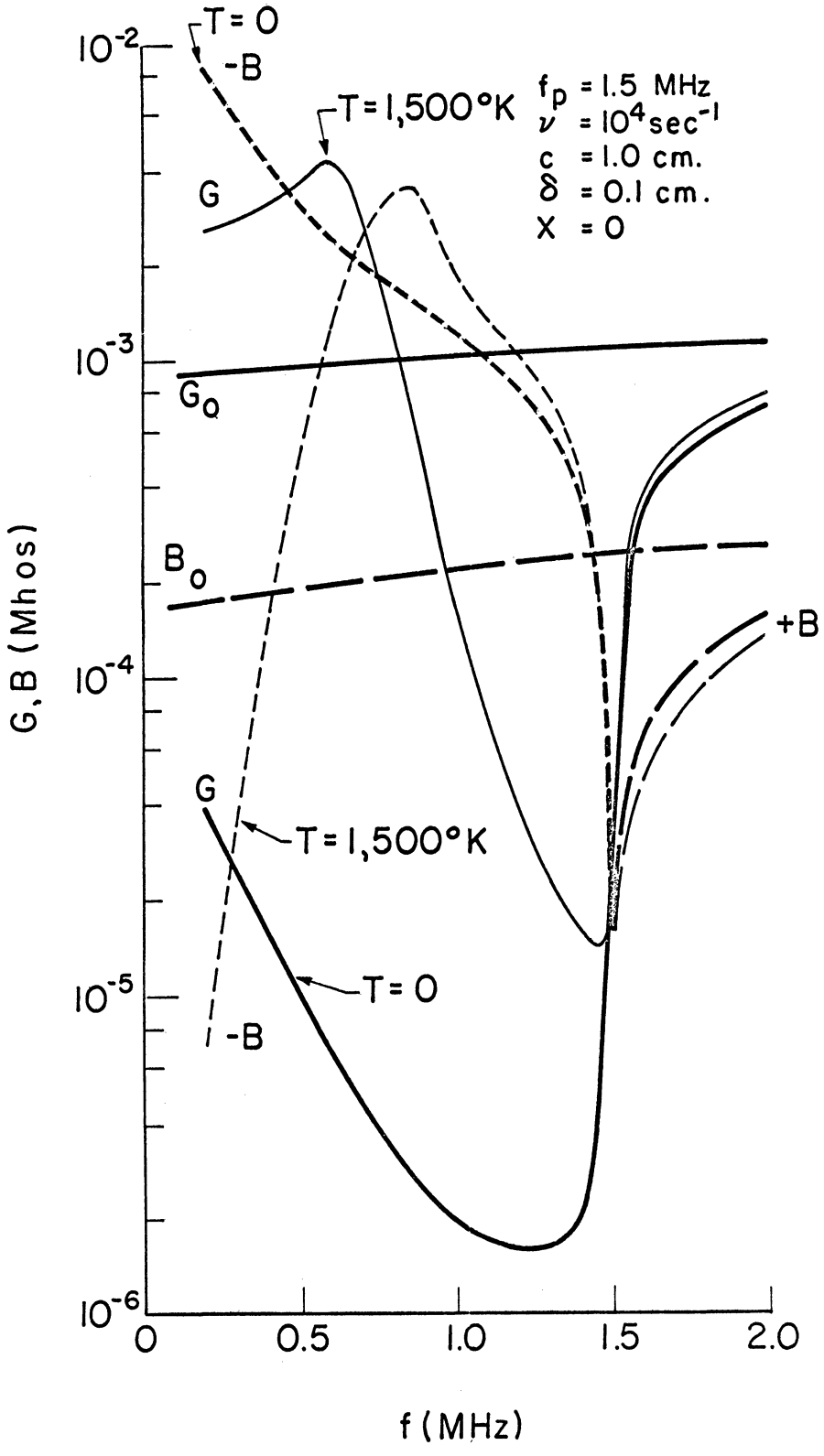

Figure 8. The infinite antenna admittance as a function of frequency in an isotropic plasma for both the compressible (T=1, 500°K) and incompressible (T=0°K) cases and zero sheath thickness with an electron plasma frequency of 1.5 MHz.

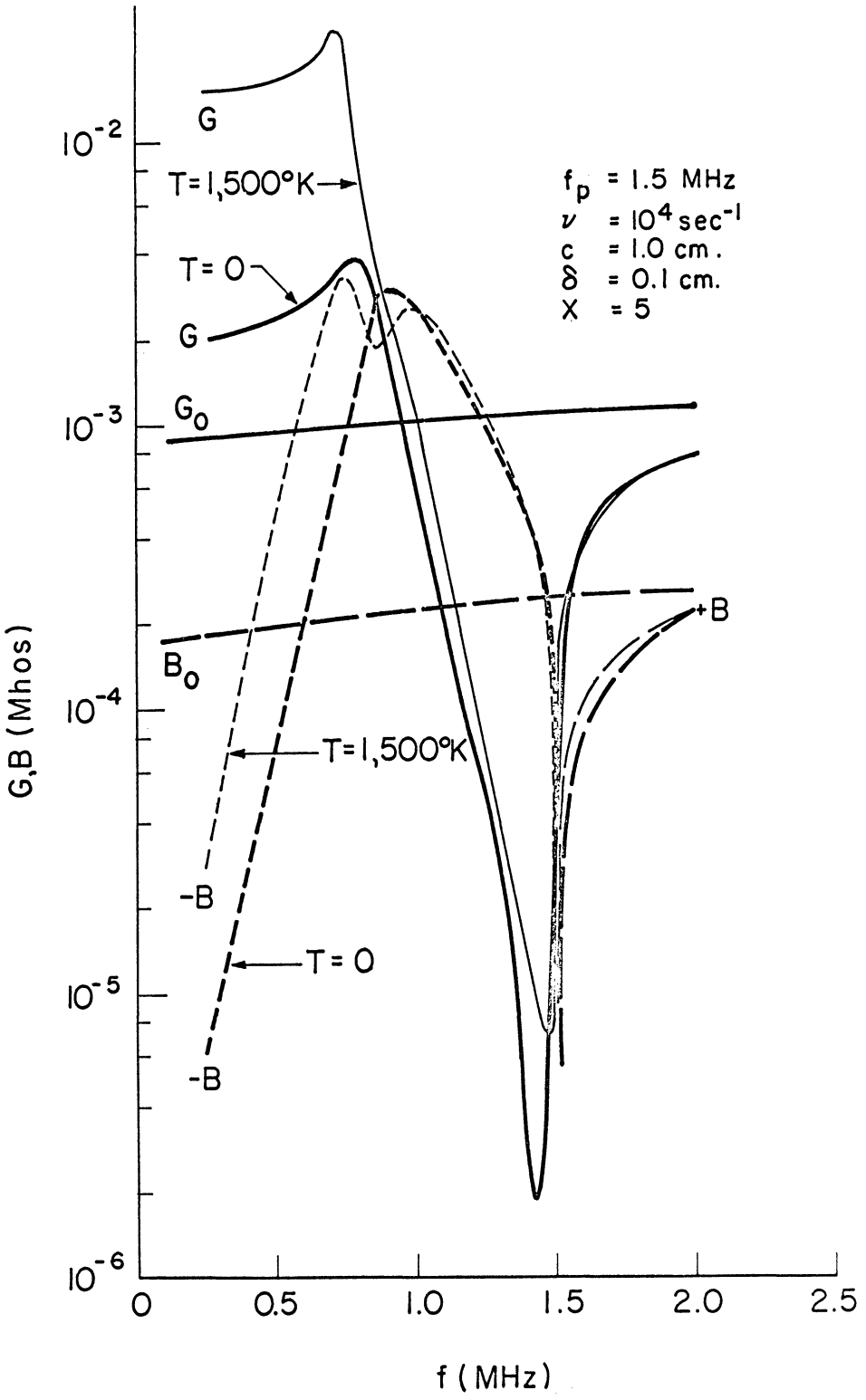

Figure 9. The infinite antenna admittance as a function of frequency in an isotropic plasma for both the compressible (T=1, 500°K) and incompressible (T=0°K) cases and a vacuum sheath thickness of 5 D_ℓ with an electron plasma frequency of 1.5 MHz.

Thus we present in Figs. 10 and 11 the circumferential antenna current, at $z = \delta/2$, for the same plasma parameters used for Figs. 2 and 3 respectively. The quantity plotted is $I = R + i\,I$, the current density K_ϕ multiplied by $2\pi c$, so that a direct numerical comparison with the axial current is meaningful. It is interesting to see that the circumferential current magnitude is generally 1 to 2 orders of magnitude less than the corresponding axial current. As might be expected, the circumferential current is largest near f_h, appearing to reach its maximum value at the same frequency as does the axial current. It is also interesting to see that the circumferential current exhibits minima or "kinks" at $f = f_p$ in a fashion similar to that shown by the axial current.

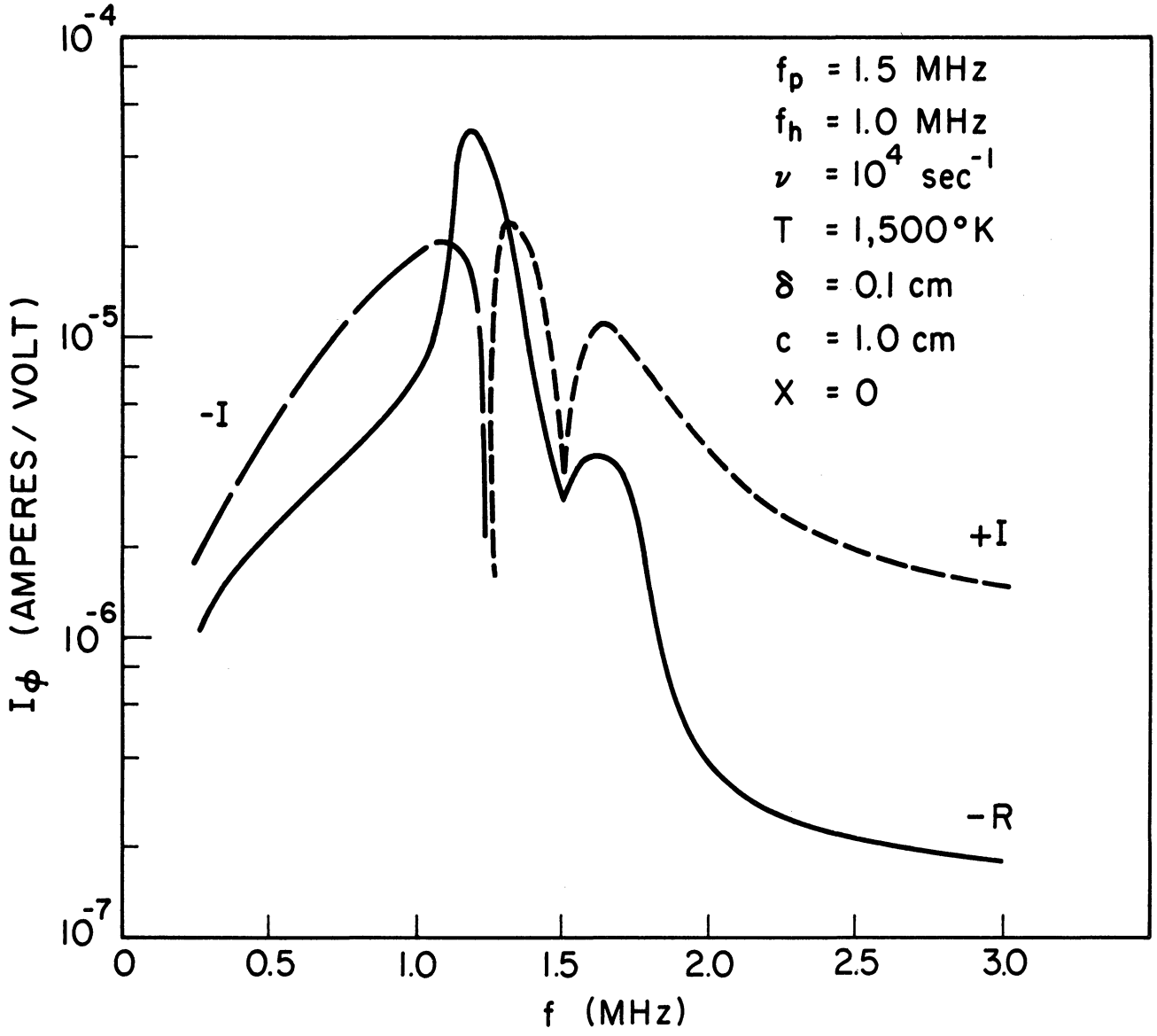

Figure 10. The circumferential current as a function of frequency for the compressible magnetoplasma and the sheathless case with an electron plasma frequency of 1.5 MHz and electron cyclotron frequency of 1.0 MHz.

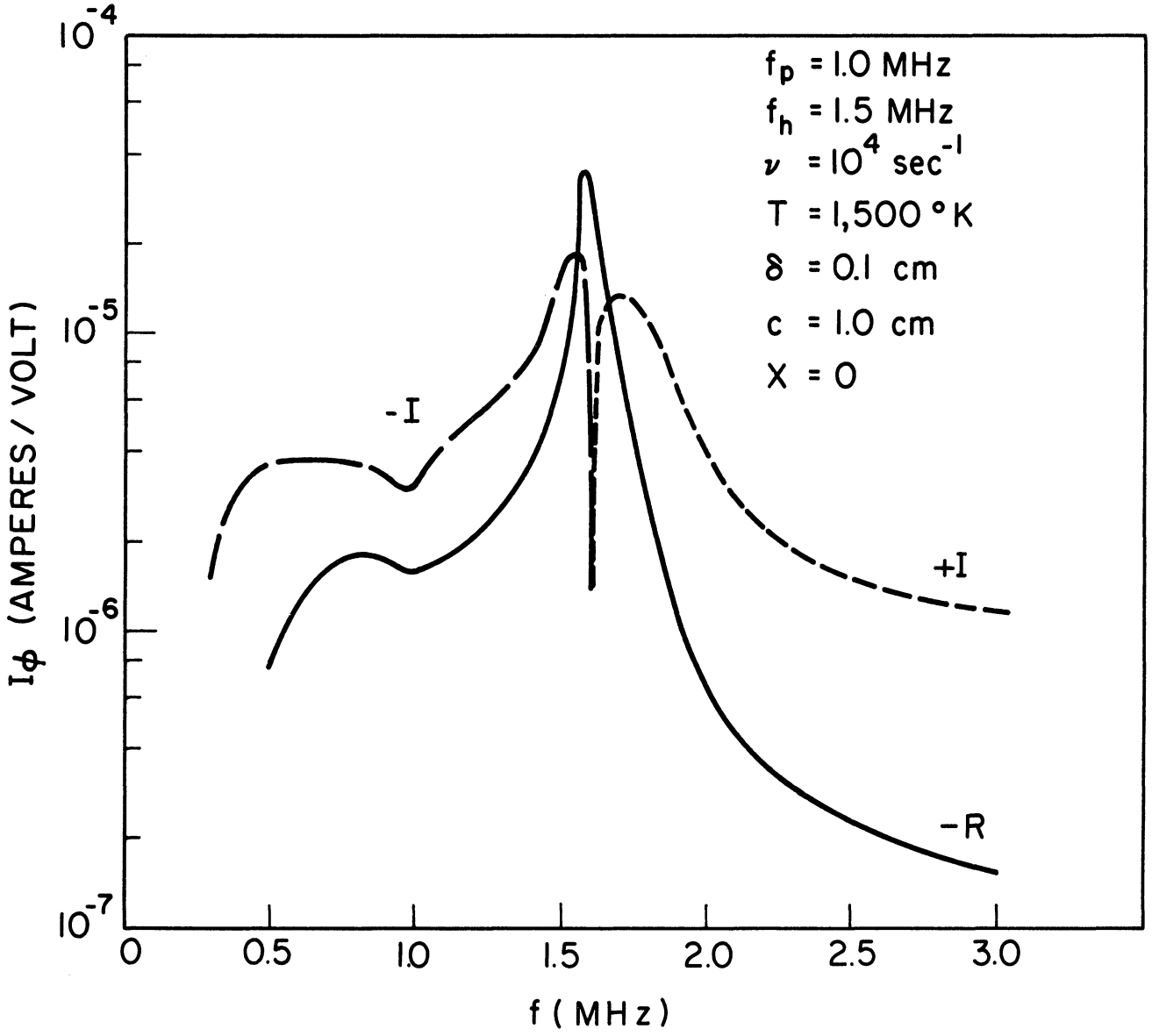

Figure 11. The circumferential current as a function of frequency for the compressible magnetoplasma and the sheathless case with an electron plasma frequency of 1.0 MHz and electron cyclotron frequency of 1.5 MHz.

IV. Comparison with Experimental Results

While this study has been devoted to an investigation of the plasma-immersed, infinite cylindrical antenna because of a number of theoretical considerations, the ultimate goal of coming to a better understanding of an actual antenna immersed in the ionospheric plasma has not been forgotten. The rationale which has been followed is that the medium influence which is apparent in the change of the infinte antenna admittance from its free space behavior, would provide a general indication of the corresponding behavior of the finite antenna in the same plasma medium. In line with this, it was anticipated that some swept-frequency experimental impedance results would be available from a rocket-borne antenna which would provide some extremely useful data for comparison with the theoretical findings presented here, as well as with some simpler theories of finite antenna impedance in the literature. It may be mentioned that there is a scarcity of systematic ionospheric impedance measurements now available for comparison with theory. With the exception of a series of rocket flights by Heikkila et. al. (1966), most published impedance data is for a series of fixed frequencies, which means that an impedance vs. frequency plot for a constant set of plasma parameters is not available. The above-mentioned experiment was designed in part to fill this gap.

The first rocket which carried this experiment was successfully launched to an altitude of 290 Km, and about 75 swept-frequency impedance records, from 800 KHz to 8 MHz, together with other related data, have been obtained from it. This data is presently being reduced and analyzed, and includes in addition to the impedance measurement, a transmission experiment, a relaxation resonance experiment, a conventional Langmuir probe and simultaneous ionosonde record, which should be extremely useful in assessing varoius diagnostic techniques for electron density measurements, as well as interpreting the impedance results. These results will be reported on in the near future.

Some comments can be made however, about the numerical results obtained here compared with some of the experimental data presented in the literature. We refer in particular to the experimental impedance results of Heikkila et. al. (1966) mentioned above, for a spherical antenna, as well as the data published in a series of articles by Stone, Weber and Alexander (1966a, 1966b, 1966c) for a cylindrical antenna. There are some features exhibited by the experimental impedances which appear to correlate with the theoretical admittances presented above.

For example, one of the prominent features of the theoretical admittance curves for the magnetoplasma case is a rather sharp minimum or "kink" which occurs in either the susceptance or conductance, whichever is the larger, or possibly both together, at the plasma frequency. The results of Heikkila et. al. show a consistent susceptance discontinuity at the plasma frequency (though none is seen in the conductance), with values for f_p obtained from this indicator agreeing well with other independent measurements. A similar behavior is exhibited by Stone et. al's. impedance results when $f_p < f_h$, there being an abrupt change in the reactance and pronounced resistance peaking at $f=f_p$. When $f_p > f_h$ on the other hand, only the resistance shows a noticeable increase at $f=f_p$. It should be remarked that the results of Stone et. al. are for fixed frequencies and shown as a function of antenna altitude (or equivalently, as a function of the plasma frequency) so that an exact comparison with the theoretical results presented above, where the frequency is varied, is not possible. There is however, a qualitative similarity between the quoted experimental results and the infinite antenna theoretical results presented here as well as numerical impedance values obtained from the theory of Balmain (1966) for a finite antenna, which is discussed more fully in II.

A second characteristic which the theoretical admittance results exhibit, an admittance maximum shifted upward from f_h by either the vacuum sheath or plasma compressibility, is also observed consistently in the measurements of Heikkila et.al. This behavior of the measured admittance has led Balmain et. al. (1967) to conclude, from the application of a quasistatic theory for the antenna impedance, that a positive ion (or vacuum) sheath is responsible for the observed upward shift of the admittance maximum from f_h. As has been mentioned above, the findings from the infinite antenna analysis show that this shift may be due to either a sheath or the plasma compressibility. It seems likely that for an actual antenna in the ionosphere, the shift may be due to a combination of both effects acting together; it is impossible to now say which would exert the greater influence on the finite antenna. However, the infinite antenna results indicate that the sheath may be more effective in this role than the plasma compressibility.

Finally, the infinite antenna findings show that an admittance minimum is to be expected at the upper hybrid frequency f_t, and more specifically, the susceptance changes sign there. This behavior, it should be noted, has not been found to be shifted in frequency by the vacuum sheath or plasma compressibility. The results of Stone et. al. do posses a susceptance zero and conductance minimum in the vicinity of f_t. On the other hand, the measurements made by Heikkila et. al. do not consistently exhibit a susceptance zero at f_t, but they do however, consistently show a minimum in the admittance magnitude at f_t (according to Balmain, et. al. (1967)).

Thus, while the amount of experimental data available in the literature for comparison with our theoretical findings is limited, we see that what there is appears to agree in some fairly significant details with the theoretical results. It is hoped that when the data from the rocket shot mentioned previously is reduced that a more detailed comparison between experiment and theory will be possible.

V Conclusion

This report has presented a theoretical development and numerical calculations for the admittance of an infinite cylindrical antenna excited at a circumferential gap of non-zero thickness and immersed in a lossy, compressible magnetoplasma, with the static magnetic field parallel to the antenna axis. Numerical values for the antenna admittance have been obtained by a numerical integration of the Fourier integral for the antenna current evaluated at the exciting gap, and are presented for plasma parameter values typical of the E-region of the ionosphere. A vacuum sheath model and inhomogeneous sheath model have been considered in the analysis, but due to the complexity and thus time-consuming nature of the calculations, the numerical results are given for the sheathless case only. In addition to giving results for the antenna admittance, which requires evaluation of the axial antenna current, some results have also been presented for the circumferential current. Finally, the most significant aspects of the calculated admittance are compared with some experimental measurements made with antennas operated in the ionosphere.

The infinite antenna admittance results presented here for the sheathless, compressible magnetoplasma case show that, compared with the incompressible magnetoplasma results, the plasma compressibility in the former case and the vacuum sheath in the latter case influence the antenna admittance in very similar ways. In particular, an admittance maximum which occurs at the electron cyclotron frequency when there is no sheath and the magnetoplasma is incompressible, is shifted upward in frequency and reduced in magnitude by both the vacuum sheath and plasma compressibility. This effect is more pronounced when $f_p > f_h$ then for the converse situation. Other than this significant

change, the sheathless magnetoplasma admittances for both the compressible and incompressible cases are very similar.

The antenna susceptance is found to be, broadly speaking, inductive when $f_h < f < f_t$ and capacitive otherwise. Besides the admittance maximum near f_h, a second maximum occurs just above f_p when $f_p > f_h$, with a rather sharp minimum in both the conductance and susceptance at f_p. When $f_p \leq f_h$, there is a susceptance maximum only just above f_p, with a conductance minimum just below this.

Above the upper hybrid frequency, the antenna admittance is not greatly affected by the plasma compressibility, anisotropy or vacuum sheath, while only when all of these factors are absent is there no admittance maximum below f_t. Of these three factors, the magnetic field, sheath and plasma compressibility, the first two appear to exert the greatest influence on the infinite antenna admittance when immersed in a plasma.

A comparison of the theoretical admittance values for the infinite antenna which have been given here with some experimental measurements performed in the ionosphere, reveals that the theoretical and experimental results are qualitatively alike in some significant details. The location of an admittance maximum above the electron cyclotron frequency, an admittance minimum or kink at the electron plasma frequency, and an admittance minimum at the upper hybrid frequency are all features that appear in both the experimental and theoretical results. The theoretical study which has been carried out thus appears to incorporate in it at least some of the more important physical processes which act on an actual antenna in an ionospheric-type plasma and may thus provide more insight into the interpretation of the rather extensive experimental program of impedance measurements which has been started.

At the same time, the relative success of the theory thus far used in accounting for the pertinent aspects of the expected experimental measurements should give more positive indication of what are the major physical processes involved, and what modifications could be incorporated in the theory, e.g., considering an inhomogeneous sheath, to bring the theory and experiment into closer agreement. Finally, it would be hoped that the major physical processes thus established may be used in developing a theory for the plasma-immersed finite antenna, possibly by a direct formulation of the problem in an appropriate finite geometry, or by extending the infinite antenna analysis through the use of multiply reflected currents on a finite antenna, as done by Chen and Keller (1962) for free space.

Appendix A

The reduction of the non-zero temperature magnetoplasma equations to those for the zero temperature magnetoplasma when the limit T→0 is used in the former equations is shown here. The warm plasma equations are given in the text by (18) to (20) and when the limit T→0 is used, these equations reduce to (21) to (23). Our problem is to reduce (21) to (23) to the form derived directly from the zero temperature equations, as was done in II, the equations for which are given by (24) and (25).

Upon substituting (23) into (21) and (22) we obtain

$$\nabla_\rho^2 \tilde{\tilde{h}}_z + (K_{Eo}^2 \epsilon_3 - \beta^2)\, \tilde{\tilde{h}}_z + i\beta \epsilon_o \frac{XY}{U^2}\, \tilde{\tilde{e}}_z + \frac{\omega Y \epsilon_o}{U \epsilon_1} \left[\frac{i\beta XY^2}{U(U^2-Y^2)}\, \tilde{\tilde{e}}_z - i\omega\mu_o \epsilon' h_z \right] = 0 \qquad \text{(A1)}$$

$$\nabla_\rho^2 \tilde{\tilde{e}}_z + (K_{Eo}^2 \epsilon_3 - \beta^2)\, \tilde{\tilde{e}}_z + \frac{i\beta}{\epsilon_1} \left[\frac{i\beta XY^2}{U(U^2-Y^2)}\, \tilde{\tilde{e}}_z - i\omega\mu_o \epsilon' \tilde{\tilde{h}}_z \right] = 0 \qquad \text{(A2)}$$

These reduce to

$$\nabla_\rho^2 \tilde{\tilde{h}}_z + (K_{Eo}^2 \epsilon_3 - \beta^2)\, \tilde{\tilde{h}}_z - K_{Eo}^2\, Y \frac{\epsilon'}{\epsilon_1 U}\, \tilde{\tilde{h}}_z + i\beta\omega\epsilon_o\, X \frac{Y}{U^2} \left[1 + \frac{Y^2}{\epsilon_1 (U^2-Y^2)} \right] \tilde{\tilde{e}}_z = 0 \qquad \text{(A3)}$$

$$\nabla_\rho^2 \tilde{\tilde{e}}_z + (K_{Eo}^2 \epsilon_3 - \beta^2)\, \tilde{\tilde{e}}_z - i\beta^2 Y \frac{\epsilon'}{U\epsilon_1}\, \tilde{\tilde{e}}_z + \beta\omega\mu_o \frac{\epsilon'}{\epsilon_1}\, \tilde{\tilde{h}}_z = 0 \qquad \text{(A4)}$$

The $\tilde{\tilde{e}}_z$ term in the $\tilde{\tilde{h}}_z$ equation can be written as

$$i\beta\epsilon_o\omega X \frac{Y}{U^2} \left[1 + \frac{Y^2}{\epsilon_1 (U^2-Y^2)} \right] = i\beta\epsilon_o\omega X \frac{Y\epsilon_3}{\epsilon_1 (U^2-Y^2)}$$

and thus

$$\left[\nabla_\rho^2 + K_{Eo}^2 \epsilon_3 - \beta^2 \left(1+i\ \frac{Y\epsilon'}{U\epsilon_1}\right)\right] \tilde{\tilde{e}}_z + \beta\omega\mu_o\ \frac{\epsilon'}{\epsilon_1}\ \tilde{\tilde{h}}_z = 0 \qquad \text{(A5)}$$

$$\left[\nabla_\rho^2 + K_{Eo}^2 \left(\epsilon_3 - i\ \frac{Y\epsilon'}{U\epsilon_1}\right) - \beta^2\right] \tilde{\tilde{h}}_z + i\beta\omega\epsilon_o X\ \frac{Y\epsilon_3}{\epsilon_1(U^2-Y^2)}\ \tilde{\tilde{e}}_z = 0 \qquad \text{(A6)}$$

It was shown in II that a direct derivation of the zero temperature magnetoplasma equations from

$$\nabla x \underline{\tilde{\tilde{e}}} = -i\omega\mu_o \underline{\tilde{\tilde{h}}}$$

$$\nabla x \underline{\tilde{\tilde{h}}} = i\omega\epsilon_o \underline{\underline{\epsilon}} \cdot \underline{\tilde{\tilde{e}}}$$

produces

$$\left[\nabla_\rho^2 + K_{Eo}^2 \epsilon_3 - \beta^2\ \frac{\epsilon_3}{\epsilon_1}\right] \tilde{\tilde{e}}_z + \beta\omega\mu_o\ \frac{\epsilon'}{\epsilon_1}\ \tilde{\tilde{h}}_z = 0 \qquad \text{(A7)}$$

$$\left[\nabla_\rho^2 + K_{Eo}^2 \left(\epsilon_1 + \frac{\epsilon'^2}{\epsilon_1}\right) - \beta^2\right] \tilde{\tilde{h}}_z - \beta\omega\epsilon_o\epsilon'\ \frac{\epsilon_3}{\epsilon_1}\ \tilde{\tilde{e}}_z = 0 \qquad \text{(A8)}$$

Some of the terms in these equations are identical and thus check. The others must be shown to be the same. Now

$$1 + i\ \frac{Y\epsilon'}{U\epsilon_1} = \frac{1}{\epsilon_1}\left[\epsilon_1 + i\ \frac{Y\epsilon'}{U}\right]$$

$$= \frac{1}{\epsilon_1}\left[1 - \frac{X}{(U^2-Y^2)} + \frac{XY^2}{U(U^2-Y^2)}\right]$$

$$= \frac{1}{\epsilon_1}\left[1 - \frac{X}{U}\right] = \frac{\epsilon_3}{\epsilon_1}$$

so the differential equation for $\tilde{\tilde{e}}_z$ checks. In addition,

$$i\omega\epsilon' = \frac{\omega XY}{(U^2-Y^2)}$$

so

$$i\beta\omega\epsilon_o X \frac{Y\epsilon_3}{\epsilon_1(U^2-Y^2)} = -\beta_o\omega\epsilon' \frac{\epsilon_3}{\epsilon_1}$$

and the $\tilde{e}_z$ part of the h_z equation also checks. Finally,

$$\epsilon_3 - i\frac{Y\epsilon'}{U\epsilon_1} = \epsilon_1\left[1 + i\frac{Y\epsilon'}{U\epsilon_1}\right] - i\frac{Y\epsilon'}{U\epsilon_1}$$

$$= \epsilon_1 + i\frac{Y\epsilon'}{U\epsilon_1}(\epsilon_1 - 1)$$

and since

$$\epsilon_1 - 1 = -i\frac{U}{Y}\epsilon'$$

then

$$\epsilon_3 - i\frac{Y\epsilon'}{U\epsilon_1} = 1 + \frac{\epsilon'^2}{\epsilon_1}$$

so that the $\tilde{\tilde{h}}_z$ wave equation also checks for both derivations.

Another limiting process of interest is the case of the uniaxial plasma, where $Y \rightarrow \infty$. In this case then (18) to (20) simplify in the following way. Since Y multiplies the $\tilde{\tilde{e}}_z$ and $\tilde{h}_z$ terms in the h_z equation, then in order that $\tilde{\tilde{h}}_z$ remain finite, the terms multiplied by Y must cancel. This means that

$$\tilde{\tilde{e}}_z = \beta\frac{iqU}{\epsilon_o X}\left(1 - \frac{\beta^2 v_r^2}{\omega^2 U}\right)\tilde{\tilde{n}} \qquad \text{(A9)}$$

which may also be deduced from the equation for $\tilde{\tilde{n}}$. We then obtain, since $\tilde{\tilde{n}}$ and $\tilde{\tilde{e}}_z$ are linearly related, only two wave equations, which are

$$\nabla_\rho^2 \tilde{\tilde{h}}_z + (K_{Eo}^2 \epsilon_3 - \beta^2)\, \tilde{\tilde{h}}_z = 0 \tag{A10}$$

$$\nabla_\rho^2 \tilde{\tilde{e}}_z + \left[(K_{Eo}^2 \epsilon_3 - \beta^2) + \frac{\beta^2 X}{U} \frac{\left(1 - \dfrac{K_{Eo}^2 v_r^2}{\omega^2 U}\right)}{\left(1 - \dfrac{\beta^2 v_r^2}{\omega^2 U}\right)} \right] \tilde{\tilde{e}}_z = 0 \tag{A11}$$

Because of the limit $Y \longrightarrow \infty$, it may be verified from (14) that $\tilde{\tilde{v}}_\rho$ and $\tilde{\tilde{v}}_\varphi$ become zero, as also does $\tilde{\tilde{e}}_\varphi$. Consequently, the only boundary condition remaining to be satisfied is that on $\tilde{\tilde{e}}_z$, and the number of modes radiated by the antenna reduces from three for the compressible, magneto-plasma to one for the compressible, uniaxial plasma which is the TM mode, the wave equation for which is given by (A11). The radial propagation constant for this mode is a rather complicated function of β, v_r, ϵ_3, ω and K_{Eo}.

If the zero-temperature limit is now taken in the uniaxial equation, then the only wave equation affected is (A11) which becomes

$$\nabla_\rho^2 \tilde{\tilde{e}}_z + (K_{Eo}^2 - \beta^2)\, \epsilon_3\, \tilde{\tilde{e}}_z = 0 \tag{A12}$$

This equation is the same on that obtained from (25), which applies for the incompressible magnetoplasma, when the limit $Y \longrightarrow \infty$ is taken in (25). However, the equation for $\tilde{\tilde{h}}_z$ obtained when $Y \longrightarrow \infty$ and then $v_r \longrightarrow 0$ and given by (A10) differs from that when first $v_r \longrightarrow 0$ and then $Y \longrightarrow \infty$ since (24) becomes, for $Y \longrightarrow \infty$,

$$\nabla_\rho^2 \tilde{\tilde{h}}_z + (K_{Eo}^2 - \beta^2)\tilde{\tilde{h}}_z = 0 \qquad (A10')$$

This differs from (A10) in the fact that ϵ_3 multiplies K_{Eo}^2 in (A10) but not in (A12).

The explanation for this apparent discrepancy lies in the fact that when Y = ∞, regardless of the value of v_r, $\tilde{\tilde{h}}_z$ is zero. This may be shown by noting from (14) that for an infinite static magnetic field, $\tilde{v}_\rho$ and $\tilde{v}_\varphi$, as well as $\tilde{e}_\varphi$ are zero. Then the z-component of (12) is zero on the left hand side, showing that $\tilde{\tilde{h}}_z$ is also zero. The TE (with respect to the static magnetic field direction) mode cannot be excited then in an uniaxial plasma.

References

Balmain, K. G. (1964), "The Impedance of a Short Dipole in a Magnetoplasma", IEEE Trans. on Ant. and Prop., AP-12, No. 5, 605-617.

Balmain, K. G., G. Oksiutik and J. Fejer, (1967), "RF Probe Admittance in the Ionosphere: Comparison of Theory and Experiment", 1967 Spring URSI Meeting, Ottawa, Ontario, Canada.

Chen, Y. and J. B. Keller (1962), "Current on and Input Impedance of a Cylindrical Antenna", J. of Res. NBS, Section D, 66D, No. 1, 15-21.

Heikkila, W. J., J. A. Fejer, J. Hugill, and W. Calvert, (1966), "Comparison of Ionospheric Probe Techniques", Southwest Center for Advanced Studies, Auroral Iohospheric Rept., DASS-66-5.

Miller, E. K. (1967a), "The Admittance of the Infinite, Cylindrical Antenna in a Lossy, Isotropic, Compressible, Plasma", U. of Michigan Scientific Rept. 05627-10-S.

Miller, E. K. (1967b), "The Admittance of the Infinite Cylindrical Antenna in a Lossy Plasma. II. The Incompressible Magnetoplasma", U. of Michigan Scientific Rept. 05627-11-S.

Self, S. A. (1963), "Exact Solution of the Collisionless Plasma Sheath Equation", Phys. of Fluids, 6, 1762-1768.

Stone, R. G., R. R. Weber and J. K. Alexander (1966a), "Measurement of Antenna Impedance in the Ionosphere. I. Observing Frequency Below the Electron Gyro Frequency," Planet. Space Sci., 14, 631-639.

Stone, R. G., R. R. Weber and J. K. Alexander, (1966b), "Measurement of Antenna Impedance in the Ionosphere, II. Observing Frequency Greater than the Electron Gyro Frequency," Planet. Space Sci., 14, 1007-1016.

Stone, R. G., J. K. Alexander and R. R. Weber (1966c), "Magnetic Field Effects on Antenna Reactance Measurements at Frequencies Well Above the Plasma Frequency", Planet. Space Sci., 14, 1227-1231.